Highlights

- Normal epithelial cells detect Ras-transformed neighbours expressing elevated EphA2.
- Cell-cell interaction between normal and RasV12 cells induce ephrinA-EphA2 signals.
- Differential EphA2 signalling drives RasV12 cell repulsion and contractility.
- Drosophila Eph is required to drive segregation of RasV12 cells in vivo.

eTOC Blurb

Porazinski et al. demonstrate differential Eph receptor signalling is required for the detection of Ras-transformed epithelial cells within epithelial sheets in vitro and in vivo. Cell-cell interactions with normal neighbours trigger Eph-dependent signals, which drive RasV12 cell segregation from normal cells at the single and multicellular level.

1. Cell-cell interaction
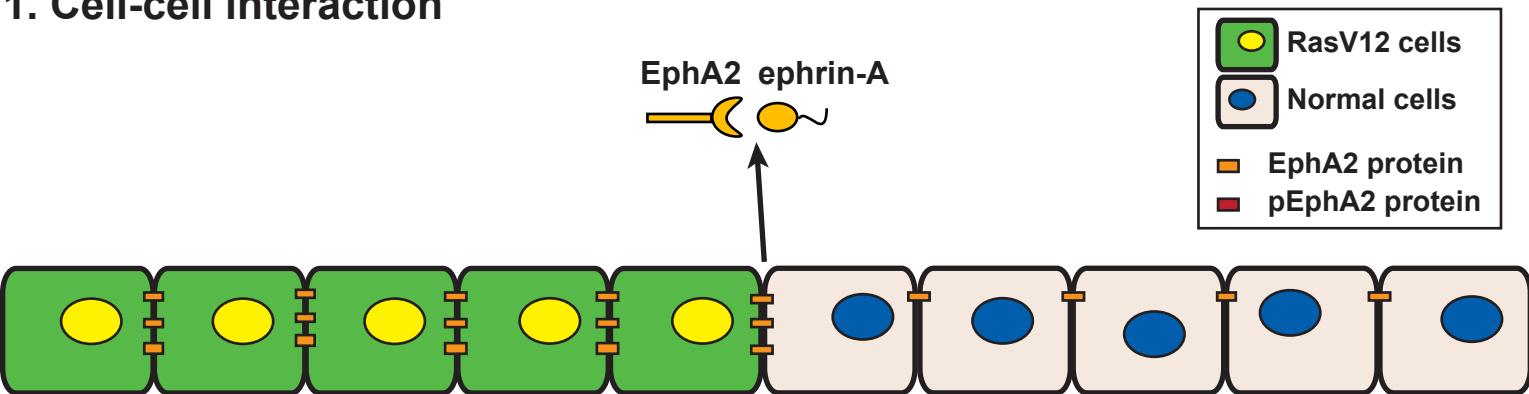
EphA2 ephrin-A

RasV12 cells
Normal cells
EphA2 protein
pEphA2 protein

2. RasV12 cell repulsion, contractility

↑ pEphA2
pSrc

actin-myosin
cytoskeleton
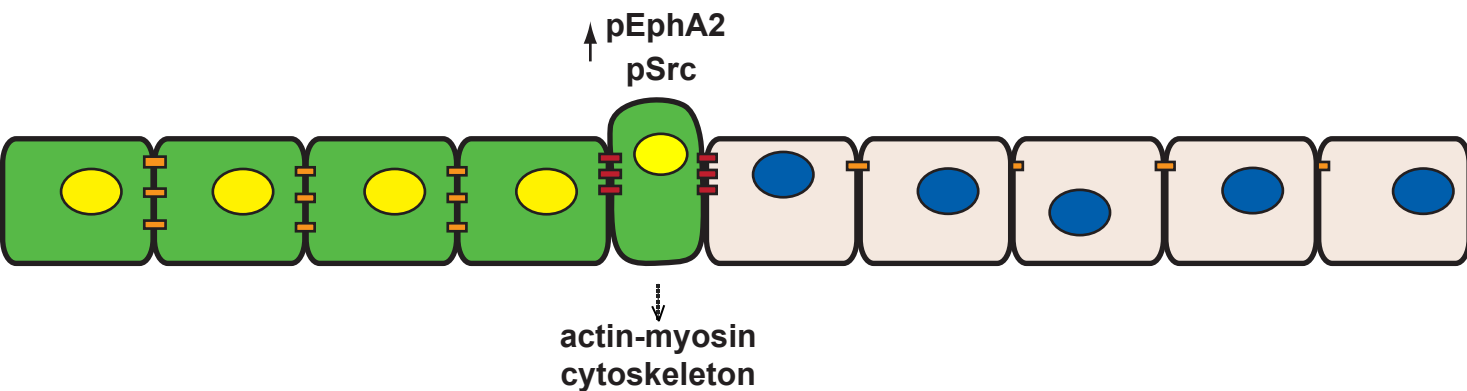
3. RasV12 cell-cell contractility
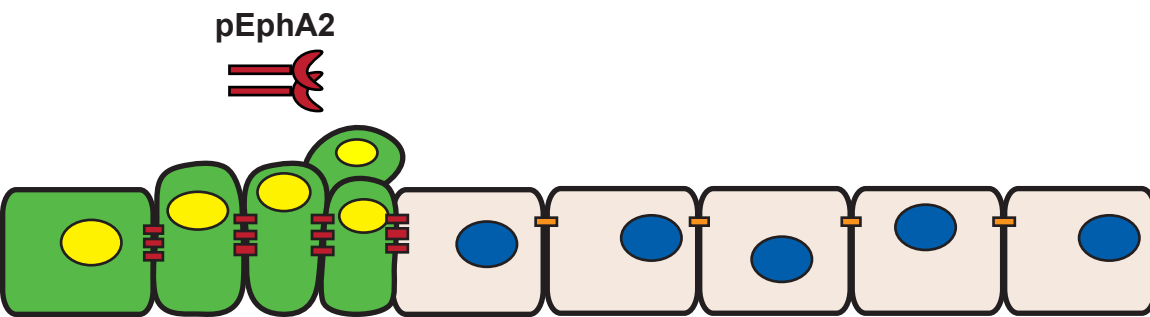
pEphA2

EphA2 drives the segregation of Ras-transformed epithelial cells from normal neighbours

Sean Porazinski[1], Joaquín de Navascués[1], Yuta Yako[2], William Hill[1], Matthew Robert Jones[1], Robert Maddison[1], Yasuyuki Fujita[2] and Catherine Hogan[1]*

[1]European Cancer Stem Cell Research Institute, Cardiff University, Hadyn Ellis Building, Maindy Road, Cardiff CF24 4HQ, UK.

[2]Division of Molecular Oncology, Institute for Genetic Medicine, Hokkaido University Graduate School of Chemical Sciences and Engineering, Kita 15, Nishi 7, Kita-ku, Sapporo, Hokkaido, 060-0815, Japan.

*Correspondence to Catherine Hogan (HoganC@cardiff.ac.uk)

Summary

In epithelial tissues, cells expressing oncogenic Ras (hereafter RasV12 cells) are detected by normal neighbours and as a result are often extruded from the tissue [1-6]. RasV12 cells are eliminated apically, suggesting that extrusion may be a tumour suppressive process. Extrusion depends on E-cadherin-based cell-cell adhesions and signalling to the actin-myosin cytoskeleton [2, 6]. However, the signals underlying detection of the RasV12 cell and triggering extrusion are poorly understood. Here, we identify differential EphA2 signalling as the mechanism by which RasV12 cells are detected in epithelial cell sheets. Cell-cell interactions between normal cells and RasV12 cells trigger ephrin-A-EphA2 signalling, which induces a cell repulsion response in RasV12 cells. Concomitantly, RasV12 cell contractility increases in an EphA2-dependent manner. Together, these responses drive the separation of RasV12 cells from normal cells. In the absence of ephrin-A-EphA2 signals, RasV12 cells integrate with normal cells and adopt a pro-invasive morphology. We also show that *Drosophila* Eph (DEph) is detected in segregating clones of RasV12 cells and is functionally required to drive segregation of RasV12 cells in vivo, suggesting that our in vitro findings are conserved in evolution. We propose that expression of RasV12 in single or small clusters of cells within a healthy epithelium creates ectopic EphA2 boundaries, which drive the segregation and elimination of the transformed cell from the tissue. Thus, deregulation of Eph/ephrin would allow RasV12 cells to go undetected and expand within an epithelium.

Results and Discussion

Based on our previous findings [2], we hypothesised that extrusion of RasV12 cells is triggered by cell-cell signals at the RasV12-normal interface. To identify these signals, we designed the 'cell confrontation assay' in order to amplify the interface between RasV12 and normal epithelial cells, and used Madin-Darby canine kidney (MDCK) epithelial cell culture systems, expressing GFP-tagged, constitutively active, oncogenic Ras (RasV12) in a tetracycline/doxycycline-inducible manner [2]. Normal or GFP-RasV12 cells were seeded into one of two compartments of a cell culture insert, separated by a fixed gap (Figure S1A), similar to [7]. After removing the culture insert, cells migrated to close the gap; opposing cells collided and cell-cell interaction occurred between marginal cells. Live cell imaging experiments revealed that upon collision with normal cells, marginal GFP-RasV12 cells collapsed (Figure S1B) and were repulsed backwards, while normal cells continued to migrate forward (Figure 1A, 1B, R:N TetON; Movie S1). At 21-30 h post-collision, RasV12 cells had tightly packed and separated from normal cells by a distinct and visible border (Figure 1A). These phenomena only occurred when GFP-RasV12 was induced in one population of cells (Figure 1B, R:N TetOFF). In contrast, when two opposing sheets of GFP-RasV12 cells collided, both populations stopped migrating (Figure 1B, R:R TetON; Movie S2) and fused to form a monolayer (Figure 1A). In the absence of cells in the second compartment, GFP-RasV12 cells continued to migrate forward into free space (Figure 1B, R:No cells). Single-cell tracking analyses confirmed that upon collision with normal cells, RasV12 cells (either at the margin or further behind the leading edge) were repulsed backwards with the same direction (Figure S1C; Movie S3). In contrast, when RasV12 cells collided with RasV12 cells, cell migration lacked directionality (Figure S1C; Movie S3). Thus, upon collision with normal cells, RasV12 cells display cell repulsion, are triggered to migrate backwards and avoid intermingling with normal cells.

Following collision with normal cells, RasV12 cells rapidly adopted a contractile morphology. We measured changes in RasV12 cell area as readout for cell contractility, and found that RasV12 cell area significantly decreased following collision with normal cells but not with RasV12 cells (Figure 1C). This decrease was observed in marginal RasV12 cells (row 1) and in RasV12 cells positioned further behind the collision interface (+11; Figure S1D). Hence, as leading RasV12 cells are repulsed,

RasV12 cells behind the margin become compressed. In contrast, RasV12 colliding with RasV12 cells maintained a constant cell area (Figure S1D).

Consistent with our previous findings [2], we observed that F-actin accumulated specifically at cell-cell contacts between RasV12 cells that had collided with normal cells (Figure 1D). Moreover, neighbouring RasV12 cells positioned behind the collision interface and not in direct contact with normal cells, also accumulated F-actin at cell-cell contacts over time (Figure 1E, S1E, S1F, S1I). Inhibition of myosin-II or Src family kinase (SFK) pathways reduced RasV12 contractility (Figure S1G). Inhibition of SFK but not myosin-II, significantly decreased RasV12 cell repulsion (Figure S1H). Indeed, collision with normal cells triggered RasV12 cells to actively migrate backwards, independent of myosin-II activity (Movie S4), similar to [8]. However, phosphorylated myosin light chain (pMLC) was detected at higher levels specifically in RasV12 cells that had collided with normal cells (Figure S1I). Although we cannot rule out that migrating normal cells also compress RasV12 cells via processes that are myosin-II-independent, our findings indicate a role for myosin-II activity in RasV12 cell repulsion. Finally, cell repulsion did not occur when RasV12 cells collided with E-cadherin-depleted cells (Distance = 0 μm, n = 2). Here RasV12 cell area was more comparable to that of RasV12 cells in a monolayer (Figure 1C). Moreover, RasV12 cells and E-cadherin-depleted cells separated via an irregular interface (Figure 1F). Thus, upon collision with normal cells RasV12 cells contract and separate via a process that is dependent on E-cadherin-based cell-cell adhesion. Crucially, these experiments demonstrate that similar phenomena occur in RasV12 cells at the single-cell [2] and multicellular level following interactions with normal cells and a dependence on specific signalling proteins is required in both contexts.

Eph-ephrin signalling regulates cell repulsion and cell segregation; processes that prevent cell mixing and drive boundary formation during tissue development and maintenance [9]. Similar to previous reports [10, 11], we found that RasV12 cells expressed EphA2 mRNA (Figure S2A) and protein (Figure S2B) at elevated levels compared to normal cells. Expression of EphA2 protein was MEK-ERK-dependent (Figure S2B). MEK-ERK signalling was also required to drive RasV12 cell extrusion [2], changes in cell area (Figure S1G) and cell repulsion (Figure S1H). Therefore, we tested whether Eph-ephrins were necessary to drive RasV12 cell repulsion. We first performed cell confrontation assays in the presence of soluble, recombinant ephrin-Fc

ligands. We reasoned that soluble ligands would interfere with endogenous Eph-ephrin signalling, similar to [12-14]. Repulsion of RasV12 cells from normal cells was significantly inhibited in the presence of ephrin-A1-Fc, -A4-Fc (Figure S2C), whereas addition of ephrin-B ligands had no effect (Figure S2C). Addition of ephrin-A1, -A4 also significantly reduced RasV12 cell contractility (Figure S2D) and promoted cell intermingling at RasV12-normal cell interfaces (Figure S2E). The inhibitory effects of long-term treatment with ephrin-A ligands may be due to EphA2 down regulation from the cell surface ([15]; data not shown). Together, these results suggest a requirement of EphA family members in RasV12 cell responses following interaction with normal cells. Both normal and RasV12 cell lines also expressed EphA1, ephrin-A1 and -A4 at similar mRNA levels (Figure S2A). Given that EphA2 is a transcriptional target of Ras-MAPK signaling [10] we focused on the functional role of EphA2 in RasV12-normal cell-cell interaction.

In general, binding of ephrin ligand triggers Eph receptor clustering and activation by phosphorylation on conserved tyrosine residues [16, 17]. We detected elevated levels of phosphorylated EphA2 (Y594) in clusters of RasV12 cells surrounded by normal cells (Figure S3A), and in RasV12 cells that had immediately collided with, and been repulsed by normal cells (Figure 1G). The intensity of phosphorylated EphA2 was significantly higher at the RasV12-normal interface (Figure S3B), demonstrating that activation of EphA2 is specifically occurring upon cell-cell interaction. Phosphorylated EphA2 was also detected at significantly higher levels at cell-cell contacts between RasV12 cells within a cluster (Figure S3B; S3F).

To test the functional role of EphA2, we established two GFP-RasV12 cell lines that constitutively expressed independent shRNA constructs targeting EphA2 (shRNA-1 or -2) as well as scramble control (Figure S3C). When cultured with normal cells at 1:100 ratios, EphA2-depleted RasV12 cells no longer clustered but appeared flat and spread (Figure 2A). As expected, we did not detect elevated levels of phosphorylated EphA2 in EphA2 depleted cells (Figure 2A). To quantify the change in cell morphology, we measured the distance between the centre of nuclei of neighbouring cells in direct contact (inter-nuclear distance, IND; Figure 2B). When surrounded by normal cells, RasV12 cells depleted of EphA2 had a significantly higher IND compared to RasV12 cells expressing scramble shRNA or parental RasV12 cells (Figure 2C), and this was more comparable to the IND value of RasV12 cells in a monolayer (Figure 2C). In confrontation assays with normal cells, RasV12 cells de-

pleted of EphA2 were repulsed less efficiently (Figure 2D) and did not decrease in cell area (Figure 2E), independent of their distance to the collision margin (Figure S1D). This demonstrates that EphA2 is functionally required to induce the contraction of RasV12 cells that are both in direct contact with normal cells and further behind the collision interface. Moreover, quantification of the linearity of the border between cells ([18]; Figure 2F), indicated that depletion of EphA2 in RasV12 cells promotes local intermingling of RasV12 cells and normal cells at the cell-cell interface. Interestingly, RasV12 cells depleted of EphA2 formed large basal protrusions at the interface with normal cells (Figure 2A, 2G, 2H), indicative of a pro-invasive morphology, also reported in [2]. F-actin did not accumulate at cell-cell contacts between RasV12 cells depleted of EphA2, either when present in normal monolayers at 1:100 ratios (Figure 2G), or following collision in confrontations assays (Figure 2H; S1E, bottom panels). Using established assays [1-5], we found that RasV12 cells depleted of EphA2 were apically extruded at a significantly lower frequency than controls (Figure 2I). Together, our data demonstrate that EphA2 expressed on RasV12 cells is activated by direct cell-cell interaction with normal cells to induce repulsion and contraction of RasV12 cells, and promote the separation of RasV12 and normal cells. Moreover, EphA2 is required to induce the contraction and clustering of juxtaposed RasV12 cells that are not in direct contact with normal cells.

As signalling via SFK and myosin-II are required for RasV12 cell contractility (Figure S1G) and extrusion [2], we asked whether these signals act downstream of EphA2 in RasV12 cells. Phosphorylated (Y416) active Src was detected at elevated levels specifically in RasV12 cells surrounded by normal cells but was absent in RasV12 cells-depleted of EphA2 (Figure S3D, S3F). In confrontation assays with normal cells, the level of pMLC was reduced in RasV12 cells depleted of EphA2 (Figure S3G). Together these data suggest that SFK and myosin-II are activated downstream of EphA2 in RasV12 cells following interaction with normal cells.

We next explored the requirement of ephrin-A ligands for RasV12 cell repulsion. Since normal cells express ephrin-A1 and -A4 ([11]; Figure S2A), we focused on examining the role of these specific ligands, firstly by using the cell confrontation assay. We used preclustered ephrin-A1-Fc/-A4-Fc (or Fc alone) to coat one compartment of the cell confrontation assay, and seeded RasV12 or normal cells in the other compartment in a modified stripe assay [19]. Preclustered recombinant ephrin-Fc proteins can induce Eph receptor clustering and activate signalling [20]. We found that

both RasV12 and normal cells migrated over Fc proteins (Figure 3A), but failed to migrate over ephrin-A1-Fc ligands (Figure 3A), indicating that both cell populations are contact-inhibited by ephrin-A1 ligands. RasV12 cells, and to lesser extent normal cells, were also contact inhibited by ephrin-A4 ligands (Figure 3A). These observations were consistent with the fact that both normal and RasV12 cells express EphA2 and EphA1 receptors, which specifically bind ephrin-A1 and/or -A4 ligands [21]. RasV12 cells depleted of EphA2 migrated (albeit weakly; most likely due to residual levels of functional EphA2 expressed on these cells; see Figure S3C) over stripes of ephrin-A1-Fc or –A4-Fc (Figure 3B), suggesting that efficient contact inhibition requires EphA2.

We predicted that upon interaction with ephrin-A ligands RasV12 cells are also triggered to cluster. To test this, we first seeded GFP-RasV12 cells sparsely (and in the presence of tetracycline/doxycycline) in order to promote cell scattering ([22]; Figure 3D, top panels), before treating the cells with preclustered Fc proteins. Stimulation with ephrin-A-Fc ligands induced RasV12 cells to decrease in cell area, tightly cluster and increase E-cadherin-based cell-cell adhesion between cells (Figure 3C). Cells treated with Fc protein appeared similar to untreated cells (compare Figure 3C to 3D). Consistently, RasV12 cells expressing EphA2 shRNA (and not scramble shRNA) did not alter cell morphology or cell-cell adhesion following stimulation with ephrin-A-Fc proteins (Figure 3D). Next, we tested whether ephrin-A ligands endogenously expressed on normal cells activate EphA2 expressed on RasV12 cells. We first treated normal cells with the enzyme phosphatidylinositol-specific phospholipase C (PI-PLC) to remove GPI-linked ephrin-A ligands [23], before mixing with RasV12 cells at 1:100 ratios. Treatment with PI-PLC significantly removed endogenous ephrin-A1 from normal cells (> 80%), which remained depleted up to 24 h after treatment (Figure 3E). The level of phosphorylated EphA2 (Y594) was markedly reduced in RasV12 cells when surrounded by PI-PLC-treated normal cells compared to RasV12 cells surrounded by PBS-treated cells (Figure 3F). RasV12 cells failed to tightly cluster in the presence of PI-PLC-treated normal cells (Figure 3G). Notably, RasV12 cells in direct contact with PI-PLC-treated normal cells formed large basal protrusions (Figure 3F), reminiscent of RasV12 cells depleted of EphA2 (Figure 2A). Taken together, our data show that ephrin-A ligands (artificially clustered or membrane bound) activate EphA2 receptor expressed on RasV12 cells and this triggers RasV12 cells to contract and cluster with increased intercellular adhesion.

Both RasV12 and normal MDCK cell lines express comparable levels of ephrin-A ligand mRNA (Figure S2A), total protein (Figure S2F) and cell surface protein (Figure S2G). However, we never observed cell repulsion between neighbouring RasV12 cells. We speculated that a difference in EphA2 expression levels between juxtaposed cells was sufficient to drive a repulsion/contractile response in the overexpressing cell. Overexpression of EphA2 in RasV12 cells could increase the cells responsiveness to exogenous ephrin ligands, similar to [24, 25]. To test this we carried out both 1:100 coculture, and cell confrontation assays using GFP-RasV12 cells and GFP-RasV12 cell lines either expressing EphA2 shRNA (EphA2 KD) or scramble shRNA. Since RasV12 EphA2 KD cells expressed low levels of EphA2 protein similar to normal cells (Figure S3C), we predicted that these cells would behave like normal cells in these experiments. Using cell confrontation assays, we found that RasV12 cells separated from RasV12 EphA2 KD cells but intermingled with RasV12 cells expressing scramble shRNA (Figure 4A). RasV12 cell area significantly decreased following collision with RasV12 EphA2 KD cells (Figure 4B), and RasV12 cells clustered with a significantly lower IND when surrounded by RasV12 EphA2 KD cells (Figure 4C). Thus, a difference in EphA2 expression levels between juxtaposed cells is sufficient to induce cell repulsion and prevent the intermingling of the opposing cells. This in turn triggers contraction and clustering of the EphA2 overexpressing cell.

Cells expressing RasV12 in wing imaginal discs of *Drosophila melanogaster* also cluster [2], with increased DE-cadherin at cell-cell contacts and form uniform clones with smooth borders [26], suggesting that similar processes also occur in vivo. Indeed, cells co-expressing GFP and RasV12 formed round clusters with smooth borders that segregate from the surrounding wild-type tissue (39.7%, n = 63; Figure 4D, 4E). In contrast, clones of cells expressing GFP were irregular in shape and did not segregate (0%, n = 102; Figure 4D, 4E). In *Drosophila*, a single Eph receptor (DEph) and ephrin ligand (Dephrin) has been identified, both of which play a role in the developing nervous system [27, 28]. DEph receptor is also required to maintain the straight shape of the anterior/posterior boundary in *Drosophila* [29]. Using purified Dephrin-Fc to probe for DEph expression, we observed a prominent increase in Fc staining within segregated RasV12 clusters but not within clones of GFP-expressing cells, (60% of segregated clones, n = 25; Figure 4D, 4E). To understand the functional

significance of this observation, we expressed RNAi constructs to silence *DEph* in RasV12 cells (Figure S4A, S4B). Depletion of DEph in RasV12 clones reduced the formation of round, cyst-like clusters that stably separated from the surrounding wild-type cells (14%, n = 176). Notably, within this population of RasV12 cells that appeared round and cyst-like, we detected elevated Dephrin-Fc staining (Figure S4C), suggesting incomplete knockdown of *DEph* in these cells. RasV12 clones expressing *DEph*-RNAi and displaying no detectable Dephrin-Fc staining, formed irregularly shaped, non-contractile clusters (Figure 4F) and were either aligned in the apico-basal axis (45%; Figure 4G), or remained attached to the basal layer (41%; Figure 4G) of the epithelium. In parallel, we induced RasV12 clones co-expressing a dominant negative *DEph* transgene (DEph DN), which consists of an extracellular and transmembrane domain but lacks the intracellular domain, including the kinase domain. Hence, DEph DN should bind ligand but would be unable to signal [30]. Similar to the RNAi lines, we observed a significant decrease in round, cyst-like clusters of RasV12 cells co-expressing DEph DN (12%, n = 103). Instead, the majority of RasV12 cells formed irregularly shaped, non-contractile clusters (88%, n = 103) (Figure 4F), which aligned in the apico-basal axis of the tissue (Figure 4G). Thus, elevated levels of DEph are detected in segregating clones of RasV12 cells and DEph is functionally required to drive the segregation of RasV12 cells from wild-type neighbours in vivo.

Epithelial cells expressing oncogenic v-Src are also extruded from normal monolayers via cell-cell interactions [3, 4]. Therefore, we asked whether EphA2 is also required for this process. We transiently expressed v-Src (or RasV12) with EphA2 dominant negative (EphA2 DN), which lacks a functional intracellular domain [31], and scored apical extrusion events. Both RasV12 and v-Src cells were extruded at significantly lower levels when cells co-expressed EphA2 DN (Figure S4D), suggesting that EphA2 signalling is also required to drive elimination of v-Src-transformed cells from epithelial cell sheets.

In summary, we have found that enhanced expression of EphA2 in RasV12 cells promotes their detection by and separation from normal neighbours. Cell-cell interactions between juxtaposed cells induce EphA2 forward signalling on RasV12 cells in an ephrin-A ligand-dependent and E-cadherin-dependent manner (Figure S4E, (1)). This triggers repulsion and an increase in cell contractility of RasV12 cells in direct contact with normal cells (Figure S4E, (2)). In turn, neighbouring RasV12 cells that are positioned behind marginal cells and not in direct contact with normal cells

are triggered to contract in an EphA2-dependent manner (Figure S4E, (3)). We cannot conclusively determine whether this step is ligand-dependent. It is possible that EphA2 receptors, which are present at elevated levels on RasV12 cell membranes, become mobile [32] to form higher order clusters in the absence of ligand, promoting autophosphorylation events [33]. Together with our previous studies, we propose that a combination of the initial repulsion signal and the concomitant contractility, promotes the segregation and extrusion of RasV12 cells from normal monolayers. Our findings demonstrate that epithelial cells detect and respond to neighbouring cells overexpressing Eph both in vitro and in vivo, and it is the steep difference in Eph expression levels between juxtaposed cells that is critical for this initial response. Intriguingly, within monolayers neighbouring RasV12 cells do not display cell repulsion. It is possible that inhibitory interactions *in cis* with coexpressed ephrin-A ligands [23, 25] occur on RasV12 cells, allowing a fraction of EphA2 receptors free to interact *in trans* with available ephrin-A ligands presented on neighbouring normal cells, similar to [24, 25]. Notably, transient expression of EphA2 alone drives apical extrusion of single epithelial cells from normal monolayers at low frequencies and at protracted time points (11% extruded at 48 h, n = 247 cells), suggesting that additional signals may be required for efficient extrusion. Based on our findings, we propose that EphA2-mediated repulsion drives the segregation of RasV12 cells from normal cells, similar to mechanisms underlying cell segregation at tissue boundaries during development [34, 35]. At ectoderm-mesoderm boundaries, local Eph-ephrin signals generate local increases in myosin-II-dependent contractility, which inhibits cadherin clustering at cell-cell interfaces [36]. Our findings are distinct from S1P-dependent mechanisms of extrusion [37, 38].

Many Eph receptors are abnormally expressed during tumorigenesis, though the significance of this deregulation at the single-cell level is poorly understood. In some cancer models, ephrin-expressing normal cells compartmentalise and suppress the expansion and invasiveness of Eph-receptor overexpressing cancer cells [39, 40]. Compartmentalisation of cancer cells and RasV12 cells requires E-cadherin-based cell-cell adhesions ([39]; Figure 1F). It is possible that under pathological conditions where E-cadherin-based cell-cell adhesions are disrupted (e.g. inflammation and injury), EphA2-ephrin-A interactions between RasV12 and normal neighbours would not occur, allowing transformed cells to go undetected and spread within an epithelium. Whether segregation of abnormal cells by the normal surrounding tissue is tumour

promoting or tumour suppressive will require further investigation and may provide key insights into early tumorigenesis in epithelial tissues.

Author Contributions

Conceptualization, C.H.; Methodology, C.H., S.P., J.deN., Y.Y., W.H., M.R.J., R.M.; Investigation, C.H. S.P., J.deN., W.H., M.R.J., R.M.; Writing – original Draft, C.H.; Writing – Review and Editing, C.H., J.deN., Y.F., S.P.; Resources (writing scripts for image analyses; *Drosophila melanogaster* experiments), JdeN.; Supervision, C.H., Y.F.

References

1. Anton, K.A., Sinclair, J., Ohoka, A., Kajita, M., Ishikawa, S., Benz, P.M., Renne, T., Balda, M., Jorgensen, C., Matter, K., et al. (2014). PKA-regulated VASP phosphorylation promotes extrusion of transformed cells from the epithelium. Journal of cell science.

2. Hogan, C., Dupre-Crochet, S., Norman, M., Kajita, M., Zimmermann, C., Pelling, A.E., Piddini, E., Baena-Lopez, L.A., Vincent, J.P., Itoh, Y., et al. (2009). Characterization of the interface between normal and transformed epithelial cells. Nature cell biology *11*, 460-467.

3. Kajita, M., Hogan, C., Harris, A.R., Dupre-Crochet, S., Itasaki, N., Kawakami, K., Charras, G., Tada, M., and Fujita, Y. (2010). Interaction with surrounding normal epithelial cells influences signalling pathways and behaviour of Src-transformed cells. Journal of cell science *123*, 171-180.

4. Kajita, M., Sugimura, K., Ohoka, A., Burden, J., Suganuma, H., Ikegawa, M., Shimada, T., Kitamura, T., Shindoh, M., Ishikawa, S., et al. (2014). Filamin acts as a key regulator in epithelial defence against transformed cells. Nature communications *5*, 4428.

5. Ohoka, A., Kajita, M., Ikenouchi, J., Yako, Y., Kitamoto, S., Kon, S., Ikegawa, M., Shimada, T., Ishikawa, S., and Fujita, Y. (2015). EPLIN is a crucial regulator for extrusion of RasV12-transformed cells. Journal of cell science *128*, 781-789.

6. Wu, S.K., Gomez, G.A., Michael, M., Verma, S., Cox, H.L., Lefevre, J.G., Parton, R.G., Hamilton, N.A., Neufeld, Z., and Yap, A.S. (2014). Cortical F-actin stabilization generates apical-lateral patterns of junctional contractility that integrate cells into epithelia. Nature cell biology *16*, 167-178.

7. Poujade, M., Grasland-Mongrain, E., Hertzog, A., Jouanneau, J., Chavrier, P., Ladoux, B., Buguin, A., and Silberzan, P. (2007). Collective migration of an epithelial monolayer in response to a model wound. Proc Natl Acad Sci U S A *104*, 15988-15993.

8. Matsubayashi, Y., Razzell, W., and Martin, P. (2011). 'White wave' analysis of epithelial scratch wound healing reveals how cells mobilise back from the leading edge in a myosin-II-dependent fashion. Journal of cell science *124*, 1017-1021.

9. Batlle, E., and Wilkinson, D.G. (2012). Molecular mechanisms of cell segregation and boundary formation in development and tumorigenesis. Cold Spring Harbor perspectives in biology *4*, a008227.

10. Macrae, M., Neve, R.M., Rodriguez-Viciana, P., Haqq, C., Yeh, J., Chen, C., Gray, J.W., and McCormick, F. (2005). A conditional feedback loop regulates Ras activity through EphA2. Cancer cell *8*, 111-118.

11. Miura, K., Nam, J.M., Kojima, C., Mochizuki, N., and Sabe, H. (2009). EphA2 engages Git1 to suppress Arf6 activity modulating epithelial cell-cell contacts. Molecular biology of the cell *20*, 1949-1959.

12. Carter, N., Nakamoto, T., Hirai, H., and Hunter, T. (2002). EphrinA1-induced cytoskeletal re-organization requires FAK and p130(cas). Nature cell biology *4*, 565-573.

13. Dobrzanski, P., Hunter, K., Jones-Bolin, S., Chang, H., Robinson, C., Pritchard, S., Zhao, H., and Ruggeri, B. (2004). Antiangiogenic and antitumor efficacy of EphA2 receptor antagonist. Cancer research *64*, 910-919.

14.   Lawrenson, I.D., Wimmer-Kleikamp, S.H., Lock, P., Schoenwaelder, S.M., Down, M., Boyd, A.W., Alewood, P.F., and Lackmann, M. (2002). Ephrin-A5 induces rounding, blebbing and de-adhesion of EphA3-expressing 293T and melanoma cells by CrkII and Rho-mediated signalling. Journal of cell science *115*, 1059-1072.

15.   Marston, D.J., Dickinson, S., and Nobes, C.D. (2003). Rac-dependent trans-endocytosis of ephrinBs regulates Eph-ephrin contact repulsion. Nature cell biology *5*, 879-888.

16.   Janes, P.W., Nievergall, E., and Lackmann, M. (2012). Concepts and consequences of Eph receptor clustering. Seminars in cell & developmental biology *23*, 43-50.

17.   Fang, W.B., Brantley-Sieders, D.M., Hwang, Y., Ham, A.J., and Chen, J. (2008). Identification and functional analysis of phosphorylated tyrosine residues within EphA2 receptor tyrosine kinase. The Journal of biological chemistry *283*, 16017-16026.

18.   Javaherian, S., D'Arcangelo, E., Slater, B., Zulueta-Coarasa, T., Fernandez-Gonzalez, R., and McGuigan, A.P. (2015). An in vitro model of tissue boundary formation for dissecting the contribution of different boundary forming mechanisms. Integr Biol (Camb) *7*, 298-312.

19.   Knoll, B., Weinl, C., Nordheim, A., and Bonhoeffer, F. (2007). Stripe assay to examine axonal guidance and cell migration. Nat Protoc *2*, 1216-1224.

20.   Davis, S., Gale, N.W., Aldrich, T.H., Maisonpierre, P.C., Lhotak, V., Pawson, T., Goldfarb, M., and Yancopoulos, G.D. (1994). Ligands for EPH-related receptor tyrosine kinases that require membrane attachment or clustering for activity. Science *266*, 816-819.

21.   Pasquale, E.B. (1997). The Eph family of receptors. Current opinion in cell biology *9*, 608-615.

22.   Potempa, S., and Ridley, A.J. (1998). Activation of both MAP kinase and phosphatidylinositide 3-kinase by Ras is required for hepatocyte growth factor/scatter factor-induced adherens junction disassembly. Molecular biology of the cell *9*, 2185-2200.

23.   Falivelli, G., Lisabeth, E.M., Rubio de la Torre, E., Perez-Tenorio, G., Tosato, G., Salvucci, O., and Pasquale, E.B. (2013). Attenuation of eph receptor kinase activation in cancer cells by coexpressed ephrin ligands. PloS one *8*, e81445.

24.   Eberhart, J., Swartz, M.E., Koblar, S.A., Pasquale, E.B., and Krull, C.E. (2002). EphA4 constitutes a population-specific guidance cue for motor neurons. Developmental biology *247*, 89-101.

25.   Kania, A., and Jessell, T.M. (2003). Topographic motor projections in the limb imposed by LIM homeodomain protein regulation of ephrin-A:EphA interactions. Neuron *38*, 581-596.

26.   O'Keefe, D.D., Prober, D.A., Moyle, P.S., Rickoll, W.L., and Edgar, B.A. (2007). Egfr/Ras signaling regulates DE-cadherin/Shotgun localization to control vein morphogenesis in the Drosophila wing. Developmental biology *311*, 25-39.

27.   Scully, A.L., McKeown, M., and Thomas, J.B. (1999). Isolation and characterization of Dek, a Drosophila eph receptor protein tyrosine kinase. Molecular and cellular neurosciences *13*, 337-347.

28.   Boyle, M., Nighorn, A., and Thomas, J.B. (2006). Drosophila Eph receptor guides specific axon branches of mushroom body neurons. Development *133*, 1845-1854.

29. Umetsu, D., Dunst, S., and Dahmann, C. (2014). An RNA interference screen for genes required to shape the anteroposterior compartment boundary in Drosophila identifies the Eph receptor. PloS one *9*, e114340.

30. Dearborn, R., Jr., He, Q., Kunes, S., and Dai, Y. (2002). Eph receptor tyrosine kinase-mediated formation of a topographic map in the Drosophila visual system. The Journal of neuroscience : the official journal of the Society for Neuroscience *22*, 1338-1349.

31. Minami, M., Koyama, T., Wakayama, Y., Fukuhara, S., and Mochizuki, N. (2011). EphrinA/EphA signal facilitates insulin-like growth factor-I-induced myogenic differentiation through suppression of the Ras/extracellular signal-regulated kinase 1/2 cascade in myoblast cell lines. Molecular biology of the cell *22*, 3508-3519.

32. Salaita, K., Nair, P.M., Petit, R.S., Neve, R.M., Das, D., Gray, J.W., and Groves, J.T. (2010). Restriction of receptor movement alters cellular response: physical force sensing by EphA2. Science *327*, 1380-1385.

33. Wimmer-Kleikamp, S.H., Janes, P.W., Squire, A., Bastiaens, P.I., and Lackmann, M. (2004). Recruitment of Eph receptors into signaling clusters does not require ephrin contact. The Journal of cell biology *164*, 661-666.

34. Rohani, N., Canty, L., Luu, O., Fagotto, F., and Winklbauer, R. (2011). EphrinB/EphB signaling controls embryonic germ layer separation by contact-induced cell detachment. PLoS biology *9*, e1000597.

35. Rohani, N., Parmeggiani, A., Winklbauer, R., and Fagotto, F. (2014). Variable combinations of specific ephrin ligand/Eph receptor pairs control embryonic tissue separation. PLoS biology *12*, e1001955.

36. Fagotto, F., Rohani, N., Touret, A.S., and Li, R. (2013). A molecular base for cell sorting at embryonic boundaries: contact inhibition of cadherin adhesion by ephrin/ Eph-dependent contractility. Developmental cell *27*, 72-87.

37. Slattum, G., Gu, Y., Sabbadini, R., and Rosenblatt, J. (2014). Autophagy in oncogenic K-Ras promotes basal extrusion of epithelial cells by degrading S1P. Current biology : CB *24*, 19-28.

38. Yamamoto, S., Yako, Y., Fujioka, Y., Kajita, M., Kameyama, T., Kon, S., Ishikawa, S., Ohba, Y., Ohno, Y., Kihara, A., et al. (2016). A role of the sphingosine-1-phosphate (S1P)-S1P receptor 2 pathway in epithelial defense against cancer (EDAC). Molecular biology of the cell *27*, 491-499.

39. Cortina, C., Palomo-Ponce, S., Iglesias, M., Fernandez-Masip, J.L., Vivancos, A., Whissell, G., Huma, M., Peiro, N., Gallego, L., Jonkheer, S., et al. (2007). EphB-ephrin-B interactions suppress colorectal cancer progression by compartmentalizing tumor cells. Nature genetics *39*, 1376-1383.

40. Guo, H., Miao, H., Gerber, L., Singh, J., Denning, M.F., Gilliam, A.C., and Wang, B. (2006). Disruption of EphA2 receptor tyrosine kinase leads to increased susceptibility to carcinogenesis in mouse skin. Cancer research *66*, 7050-7058.

Figure 1. Direct cell-cell interaction between epithelial cell sheets in a new cell confrontation assay demonstrates that normal cells trigger repulsion of RasV12 cells.

(**A**) Images extracted from a representative time-lapse cell confrontation experiment showing sheets of MDCK-pTR-GFP-RasV12 cells colliding with either normal MDCK cells (left panels), or with MDCK-pTR-GFP-RasV12 cells (right panels). Elapsed time is indicated as hours:minutes. Red line indicates point of collision. (**B**) Quantification of distance (μm) travelled by marginal RasV12 cells in cell confrontation assays. Migration distances were scored following collision of cells until the end of the experiment (42 h). Data indicate mean ± standard deviation (s.d.) from three independent experiments; *** p < 0.001 for R:N TetON versus all other conditions. (**C**) Quantification of GFP-RasV12 cell area (μm^2) in cell confrontation assays with normal cells (R:N: black bar, n = 182 cells), with GFP-RasV12 cells (R:R: white bar, n = 303 cells), or E-cadherin-depleted cells (R:E-cadherin shRNA: grey bar, n = 232 cells). Data represent mean ± s.e.m. from three independent experiments; *** p < 0.001. (**D**) Confocal images of confrontation assays. Upper panels: GFP-RasV12 cell sheets confronting normal MDCK monolayers (R:N). Lower panels: GFP-RasV12 cell sheets confronting GFP-RasV12 cells (R:R). Cells were fixed 40 h after addition of doxycycline (~16-18 h post collision) and stained with phalloidin (red) and Hoechst (blue). One population of RasV12 cells was prestained with cell tracker dye (CMTPX, magenta) to identify the boundary between the two populations of cells following collision. (**E**) Confocal images of cell confrontation assays. Upper panels: GFP-RasV12 cell sheets confronting normal MDCK monolayers (R:N); Middle panels: GFP-RasV12 cells confronting GFP-RasV12 cells (R:R); Lower panels: normal GFP-labelled cells confronting non-labelled normal MDCK cells (N:N). Cells were fixed 48-55 h after addition of doxycycline (~24-31 h post collision) and stained with phalloidin (red). (**F**) Confocal images of GFP-RasV12 cells confronting normal MDCK cells (left panel), or MDCK cells expressing E-cadherin shRNA (right panel). Cells were fixed 48 h after addition of tetracycline (~22-24 h post collision) and stained with Hoechst (blue). (**G**) Confocal images of cell confrontation assays of GFP-RasV12 cell sheets colliding with normal (non-labelled) monolayers (top panels), and GFP-RasV12 cell sheets colliding with GFP-RasV12 cells (lower panels). Cells were fixed 30 h after addition of doxycycline (~6-8 h post collision) and stained

with anti-EphA2 (grey) and anti-phospho-EphA2 (pEphA2, Y594; cyan) antibodies. Scale bar, 20 μm (**A**, **D-G**). See also **Figure S1** and **Movies S1-S4**.

Figure 2. GFP-RasV12 cells cluster, stably separate and extrude from normal epithelia in an EphA2-dependent manner.

(**A**) Confocal images of MDCK-pTR-GFP-RasV12 cells constitutively expressing either scramble shRNA (top panels) or EphA2 shRNA-1 (lower panels) mixed with normal MDCK cells at 1:100 ratios. Cells were fixed 48 h after addition of doxycycline, and stained with anti-EphA2 (grey) or anti-phospho-EphA2 (pEphA2, Y594; cyan) antibodies and Hoechst (blue). (**B**) Representative images illustrating quantification of inter-nuclear distance (IND) data using point-picker/Voronoi scripts. Nuclei were stained with Hoechst (DAPI). Images were inverted to grayscale using Fiji to ease visualisation. Upper panel: RasV12 cells in RasV12 cell monolayers (R:R). Lower panel: RasV12 cells mixed with normal cells at 1:100 ratios (R:N). (**C**) Quantification of inter-nuclear distance (IND; μm) between neighbouring GFP-RasV12 cells in single or 1:100 co-culture assays. R:N: GFP-RasV12 cells mixed with normal MDCK cells at 1:100 ratios (black bar, n = 148 measurements); R:R: GFP-RasV12 cells alone (white bar, n = 293 measurements); RScb:N: GFP-RasV12 cells constitutively expressing scramble shRNA mixed with normal MDCK cells at 1:100 ratios (light grey bar, n = 192 measurements); REphA2 KD:N: GFP-RasV12 cells constitutively expressing EphA2 shRNA-1 mixed with normal MDCK cells at 1:100 ratios (dark grey bar, n = 230 measurements). Data represents mean ± s.e.m. from three independent experiments; *** $p < 0.001$. (**D**) Quantification of distance (μm) travelled by leading edge of GFP-RasV12 cells constitutively expressing either scramble shRNA (white bar) or EphA2 shRNA-1 (black bar) following collision with normal cells (not depicted) until the end of the experiment (42 h). Data indicate mean ± s.e.m. from three independent experiments; *** $p < 0.001$. (**E**) Quantification of GFP-RasV12 cell area (μm^2) in cell confrontation assays with normal cells. White bar: MDCK-pTR-GFP-RasV12 cells constitutively expressing scramble shRNA (n = 457 cells); Black bar: MDCK-pTR-GFP-RasV12 cells constitutively expressing EphA2 shRNA-1 (n = 296 cells). Data represent mean ± s.e.m. from three independent experiments; *** $p < 0.001$. (**F**) Quantification of coefficient of boundary smoothness separating two populations of cells following collision in cell confrontations assays. R:N:

GFP-RasV12 cells colliding with normal MDCK cells (black bar, n = 55 measurements); R:R: GFP-RasV12 cells colliding with GFP-RasV12 cells (white bar, n = 14 measurements); RScb:N: GFP-RasV12 cells constitutively expressing scramble shRNA colliding with normal MDCK cells (dark grey bar, n = 9 measurements); REphA2 KD:N: GFP-RasV12 cells constitutively expressing EphA2 shRNA-1 mixed with normal MDCK cells (light grey bar, n = 10 measurements). Data represents mean ± s.e.m. from at least three independent experiments; *** $p < 0.001$ for R:N versus R:R or REphA2 KD:N. R:N versus RScb:N are not significant (n.s.) (**G**) Confocal images of MDCK-pTR-GFP-RasV12 cells constitutively expressing either scramble shRNA (upper panels) or EphA2 shRNA-1 (lower panels) mixed with normal MDCK cells at 1:100 ratios. Cells were fixed 48 h after addition of doxycycline and stained with anti-EphA2 antibody (grey) or phalloidin (red). (**H**) Confocal images of cell confrontation assays. MDCK-pTR-GFP-RasV12 cell sheets expressing either scramble shRNA (top panels) or EphA2 shRNA-1 (lower panels) confronting normal (non-labelled) MDCK monolayers. Cells were fixed 30 h after addition of doxycycline (~6-8 h post collision) and stained with anti-EphA2 antibodies (grey), phalloidin (red) and Hoechst (blue). (**I**) Quantification of apical extrusion of GFP-RasV12 cells constitutively expressing either scramble shRNA (white bar), EphA2 shRNA-1 (black bar), or EphA2 shRNA-2 (grey bar) mixed with normal cells at 1:100 ratios and seeded on collagen I gels. Cells were fixed 24 h after addition of doxycycline. Data represent mean ± s.e.m. from three independent experiments; ** $p < 0.01$. Scale bar, 20 μm (**A-B, G-H**). See also **Figure S2** and **S3**.

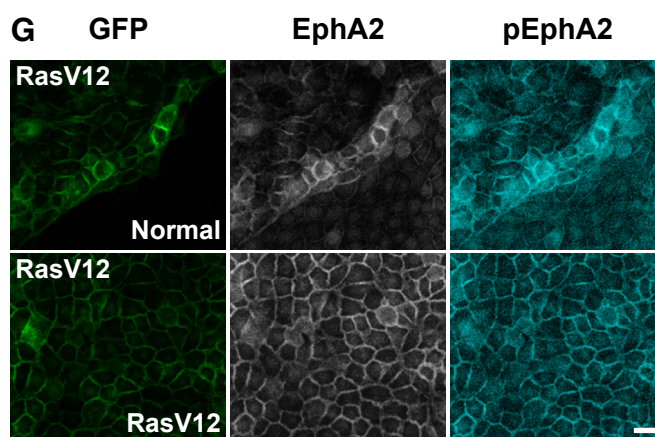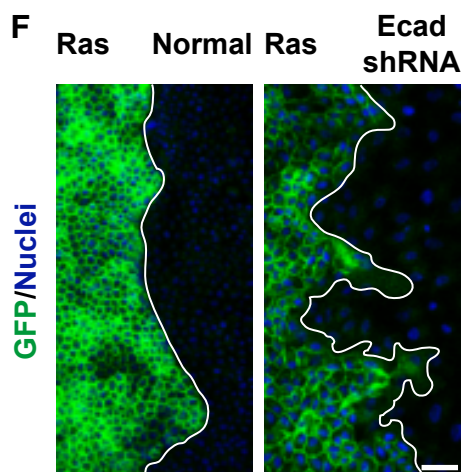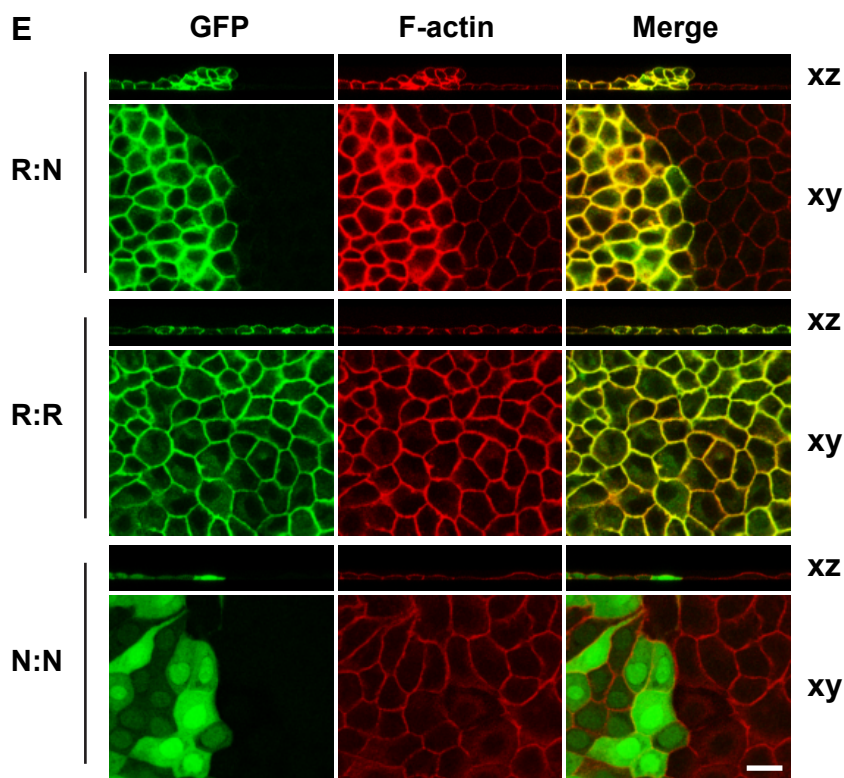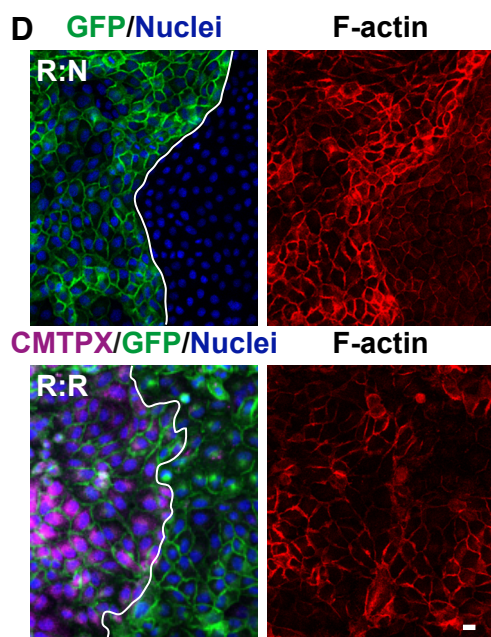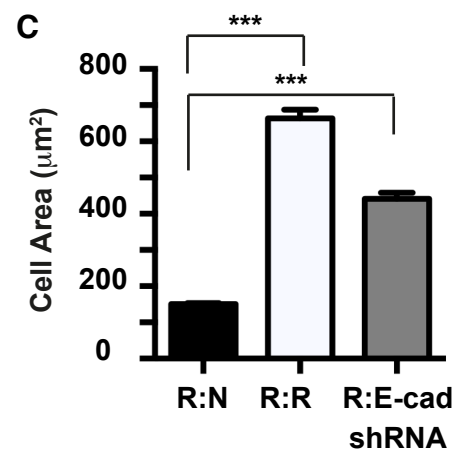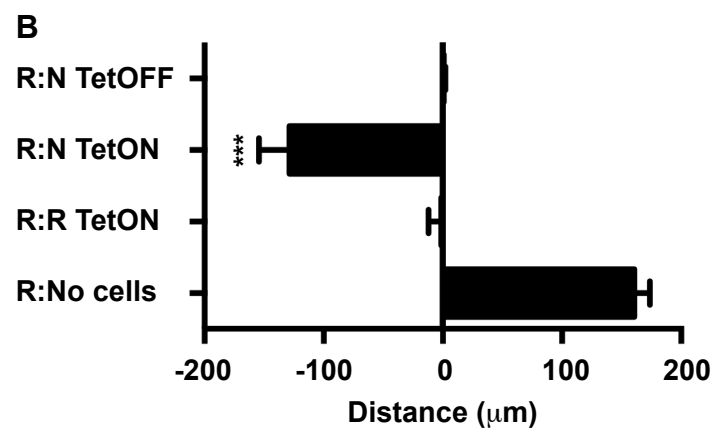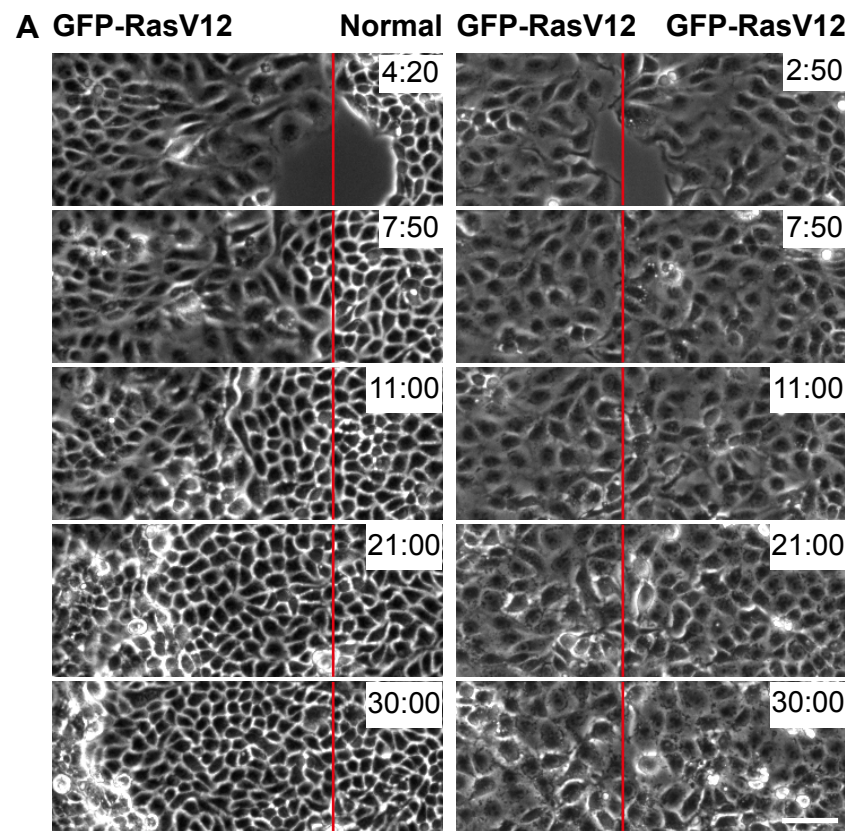**Figure 3. Ephrin-A ligands are necessary for the EphA2-dependent phenotypes in GFP-RasV12 cells.**

(**A**) Confocal images of GFP-RasV12 cells (left panels) or non-labelled, normal cells (right panels) confronting stripes of immobilised, pre-clustered Fc (top panels), ephrin-A1-Fc (middle panels) or ephrin-A4-Fc (lower panels) proteins. GFP-RasV12 cells were fixed 72 h following addition of tetracycline; normal cells were fixed at 96 h. Normal cells were stained with phalloidin (green); both cell lines were stained with Hoechst (blue). Fc protein stripes were visualised using Alexa568-conjugated anti-goat antibodies (red). Dashed white line indicates edge of each Fc protein stripe. (**B**) Epifluorescence images of MDCK-pTR-GFP-RasV12 cells constitutively expressing
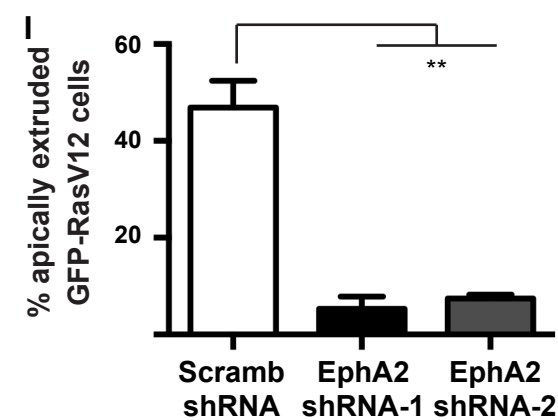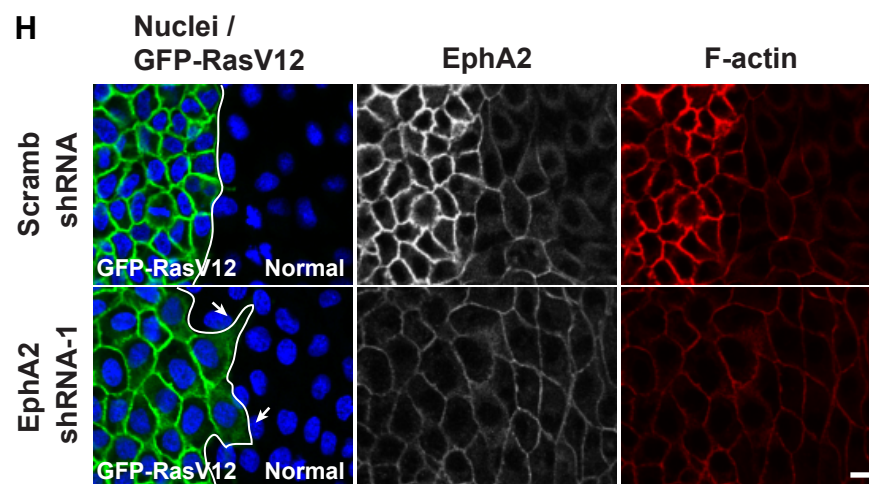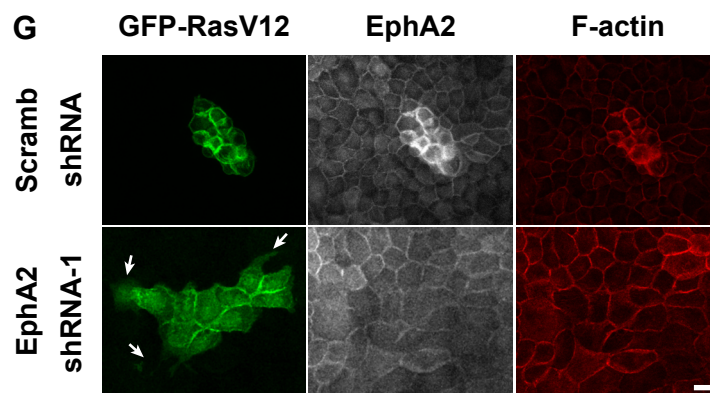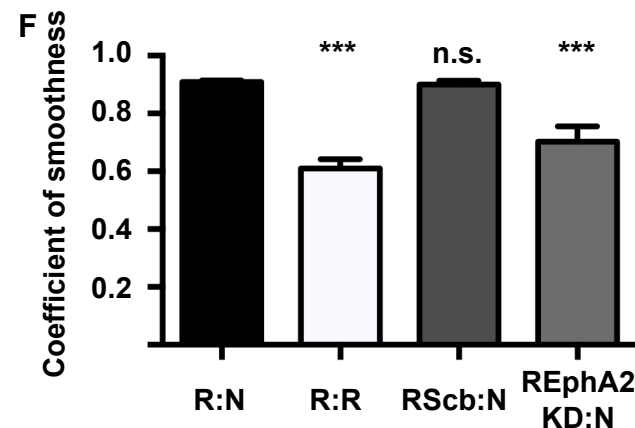
either scramble shRNA (left panels) or EphA2 shRNA-1 (right panels) confronting stripes of immobilised, pre-clustered Fc (top panels), ephrin-A1-Fc (middle panels), or ephrin-A4-Fc (lower panels) proteins. Cells were fixed 72 h following addition of doxycycline. Fc protein stripes were visualised using Alexa568-conjugated anti-goat antibodies (red). Dashed white line indicates edge of each Fc protein stripe. (**C**) Confocal images of GFP-RasV12 cells seeded at low densities, incubated overnight with doxycycline before being treated with preclustered Fc (upper panels), ephrin-A1-Fc protein (middle panels) or ephrin-A4-Fc (lower panels) (10 μg ml^{-1}) for 24 h. Cells were fixed and stained with anti-E-cadherin antibodies (cyan). (**D**) Confocal images of untreated MDCK-pTR-GFP-RasV12 cells (top panel), MDCK-pTR-GFP-RasV12 cells constitutively expressing either scramble shRNA (middle pan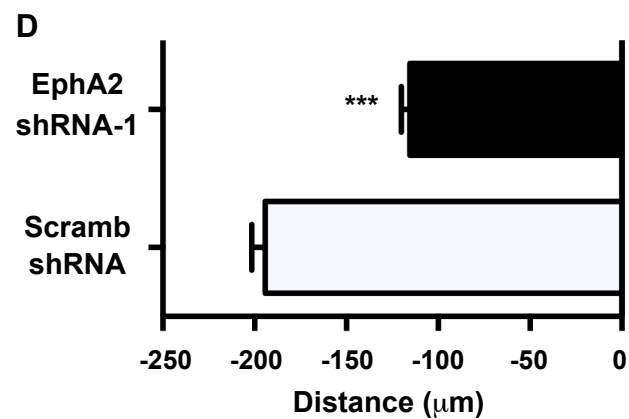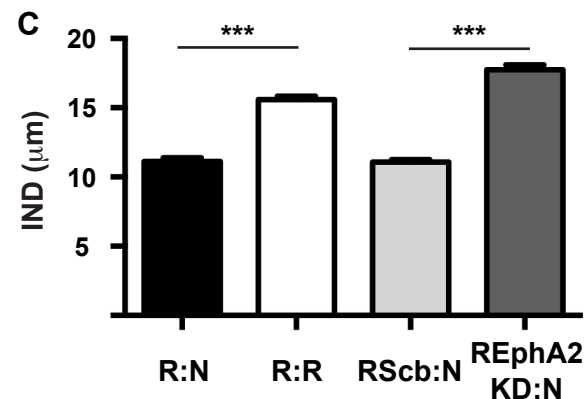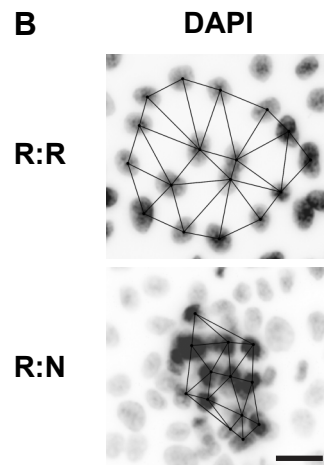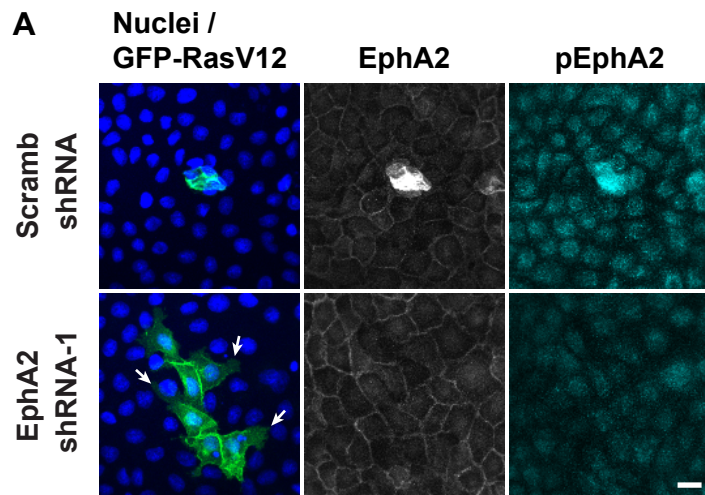els) or EphA2 shRNA-1 (lower panels). All cells were seeded at low densities and incubated overnight with doxycycline before being treated with preclustered Fc or ephrin-A1-Fc protein (10 μg ml^{-1}) for 24 h. Cells were fixed and stained with anti-EphA2 antibodies (grey), phalloidin (red) and Hoechst (blue). (**E**) Immunoblot analysis comparing the expression levels of endogenous ephrin-A1 protein from normal MDCK cell lines pre-treated with PBS (+ PBS) or phosphoinositide-specific phospholipase C (+ PI-PLC) for 4 h before being switched back to standard media for a further 24 h. Lysates were then harvested from cells and examined by Western blotting using the indicated antibodies. (**F**) Confocal images of normal MDCK cells pretreated with PBS (+ PBS: top panels) or phosphoinositide phospholipase C (+ PI-PLC: lower panels) for 4 h before mixing with GFP-RasV12 cells at 100:1 ratios. Cells were fixed 24 h after addition of doxycycline and stained with anti-EphA2 (grey), anti-phosphorylated EphA2 (pEphA2, Y594; cyan) and Hoechst (blue). (**G**) Quantification of IND (μm) between neighbouring GFP-RasV12 cells co-cultured with either untreated normal MDCK cells (Control: black bar, n = 109 measurements), normal cells pretreated with either PBS (+ PBS: grey bar, n = 88 measurements), or PI-PLC (+ PI-PLC: dark grey bar, n = 107 measurements). Data represent mean ± s.e.m. from three independent experiments; *** p < 0.001, Control versus + PBS are n.s. Scale bar, 20 μm (**A-D, F**).
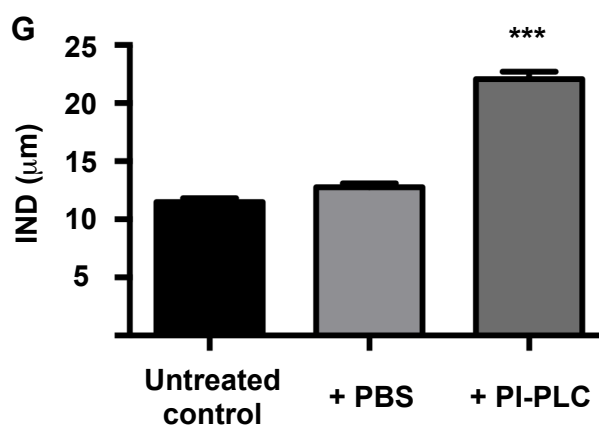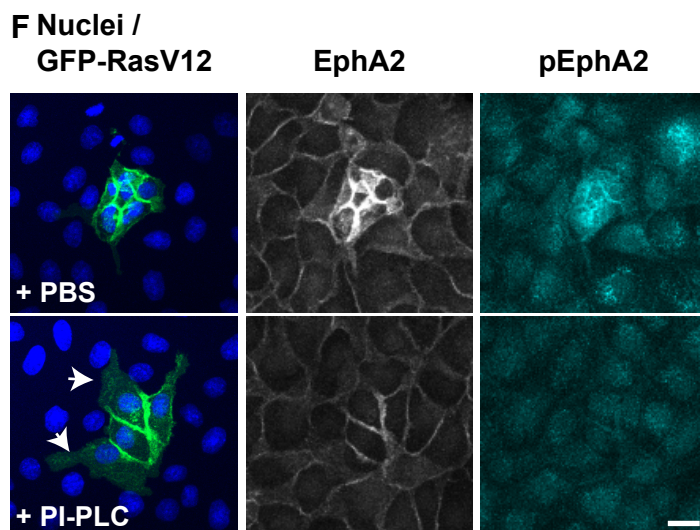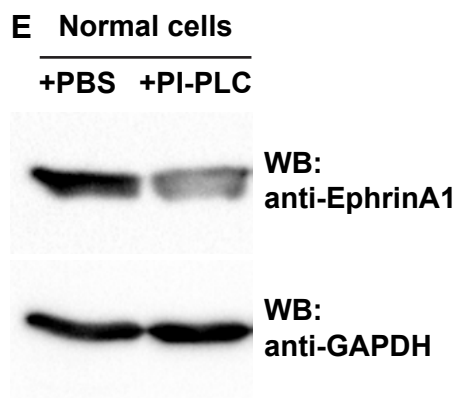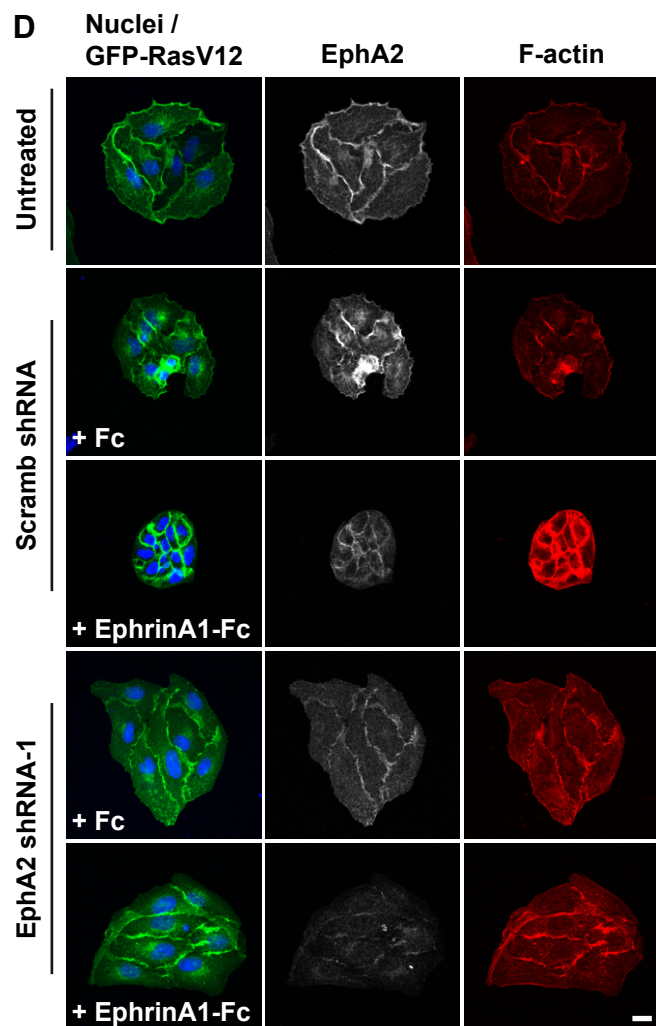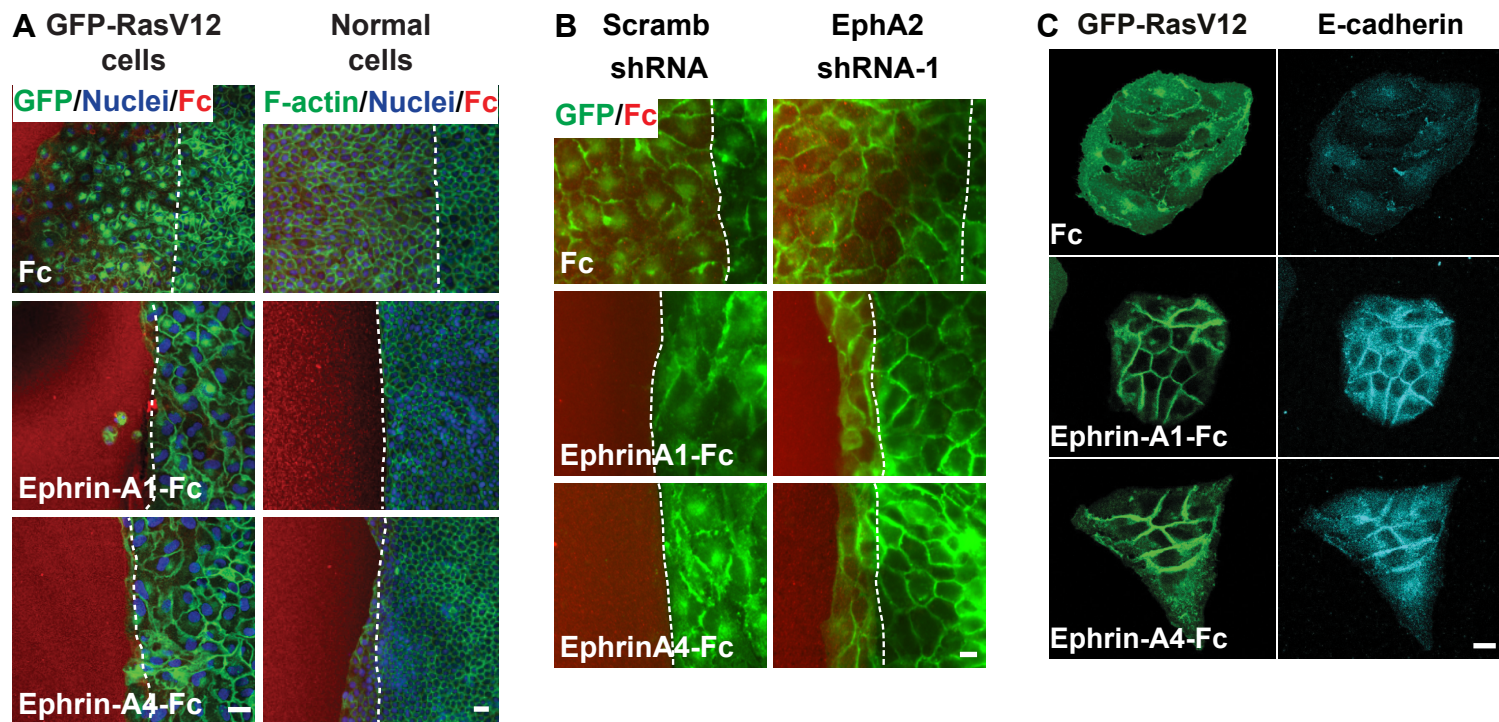
Figure 4. Neighbouring cells detect differences in Eph expression in vitro and in vivo, and this triggers segregation of the Eph overexpressing cell.
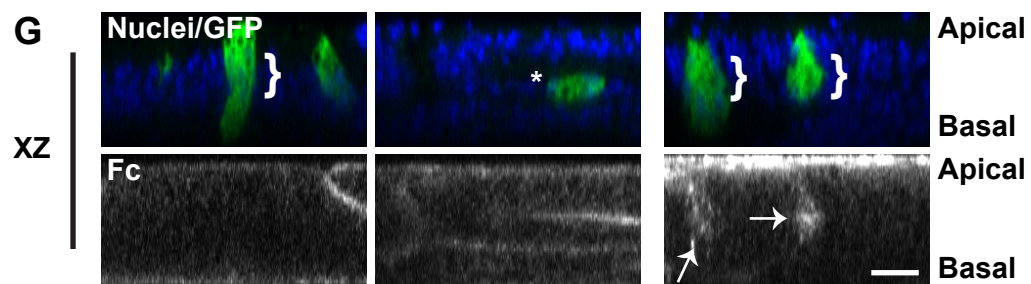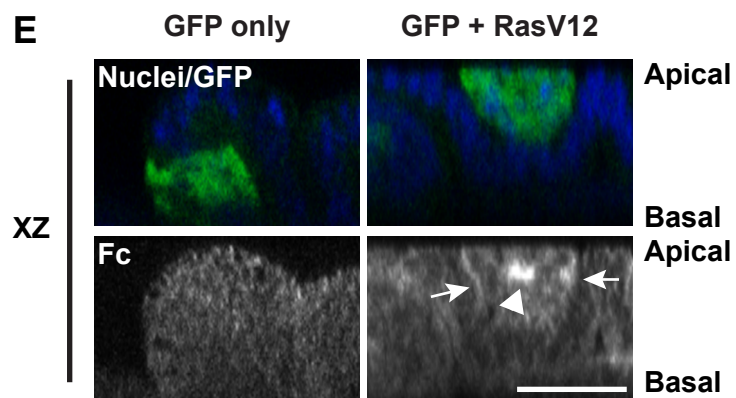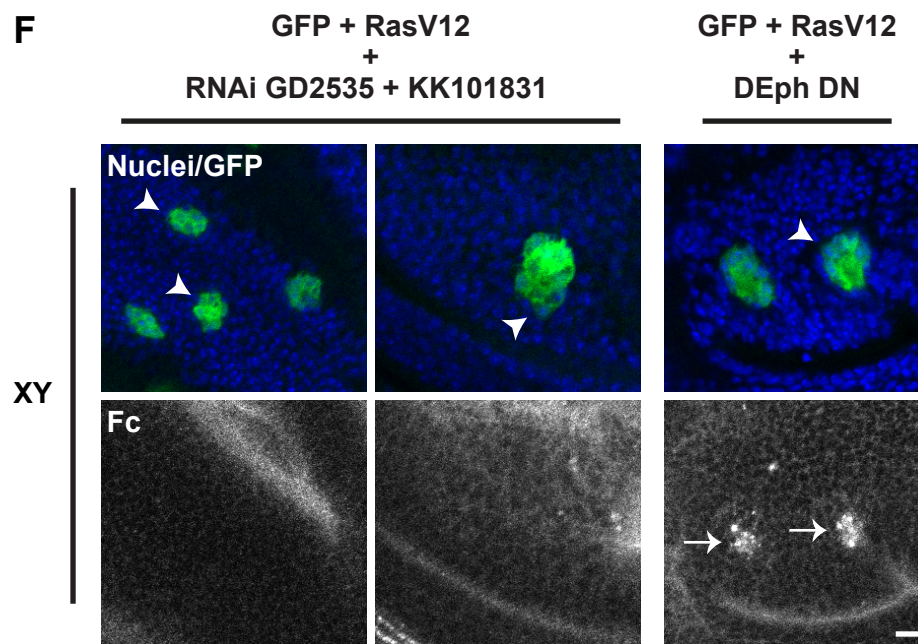
(**A**) Confocal images of cell confrontation assays. MDCK-pTR-GFP-RasV12 cell sheets expressing either scramble shRNA (top panels) or EphA2 shRNA-1 (lower panels) confronting GFP-RasV12 monolayers. GFP-RasV12 cells were prestained with CellTracker™ orange CMRA dye (red). Cells were fixed 48 h after addition of doxycycline (~22-24 h post collision) and stained with anti-EphA2 antibodies (grey) and Hoechst (blue). (**B**) Quantification of RasV12 cell area (μm^2) in cell confrontation assays with MDCK-pTR-GFP-RasV12 cells constitutively expressing scramble shRNA (Ras:Scramble: white bar, n = 756 cells), or with MDCK-pTR-GFP-RasV12 cells constitutively expressing EphA2 shRNA-1 (Ras:EphA2 KD: black bar, n = 1012 cells). Data represent mean ± s.e.m. from three independent experiments; *** $p < 0.001$. (**C**) Quantification of IND (μm) between neighbouring RasV12 cells mixed with MDCK-pTR-GFP-RasV12 cells constitutively expressing scramble shRNA (Ras:Scramble: white bar, n = 80 measurements) or with MDCK-pTR-GFP-RasV12 cells constitutively expressing EphA2 shRNA-1 (Ras:EphA2 KD: black bar, n = 95 measurements) at 1:100 ratios. Data represents mean ± s.e.m. from three independent experiments; *** $p < 0.001$. (**D**), (**E**) Confocal images of *Drosophila melanogaster* wing imaginal disc epithelia containing clones expressing GFP alone (left panels) or GFP and RasV12 (right panels). Discs were incubated with soluble Dephrin-Fc protein before being fixed and stained with anti-Fc antibody (grey) and Hoescht (blue). (**D**) XY images represent maximum projections of z-stacks. (**E**) XZ images represent an orthogonal view of a z-stack. White arrows indicate elevated ephrin-Fc staining at cell-cell contacts at the RasV12:Normal interface. White arrowhead indicates enhanced ephrin-Fc staining at the centre of the RasV12 cell cluster. (**F**) (**G**) Confocal images of *Drosophila melanogaster* wing imaginal disc epithelia containing clones coexpressing GFP and RasV12 and either two RNAi constructs (GD2535, KK101831) (left panels), or DEph dominant negative (DEph DN) (right panels). Discs were incubated with soluble Dephrin-Fc protein before being fixed and stained with anti-Fc antibody (grey) and Hoescht (blue). (**F**) XY images represent maximum projections of z-stacks. (**G**) XZ images represent an orthogonal view of a z-stack. White arrowheads indicate irregularly shaped clones of RasV12 cells. White arrows indicate punctate Dephrin-Fc staining. White asterisk indicates a RasV12 clone in contact with the basal side of the epithelium. White brackets indicate RasV12 clones

extending along the apico-basal axis of the epithelium. Scale bar, 20 μm (**A, D-G**).
See also **Figure S4**.

A GFP-RasV12 Normal GFP-RasV12 GFP-RasV12

4:20 2:50
7:50 7:50
11:00 11:00
21:00 21:00
30:00 30:00

B

R:N TetOFF
R:N TetON ***
R:R TetON
R:No cells

Distance (μm)

C

Cell Area (μm²)

R:N R:R R:E-cad shRNA

***

D

GFP/Nuclei   F-actin
R:N

CMTPX/GFP/Nuclei   F-actin
R:R

E

GFP   F-actin   Merge

R:N   xz / xy
R:R   xz / xy
N:N   xz / xy

F

GFP/Nuclei

Ras Normal Ras Ecad shRNA

G

GFP   EphA2   pEphA2

RasV12 / Normal
RasV12 / RasV12

A Nuclei / GFP-RasV12 | EphA2 | pEphA2

Scramb shRNA

EphA2 shRNA-1

B DAPI

R:R

R:N

C

IND (μm)

*** ***

R:N R:R RScb:N REphA2 KD:N

D

EphA2 shRNA-1

Scramb shRNA

***

Distance (μm)

E

Cell Area (μm²)

***

Scramb shRNA EphA2 shRNA-1

F

Coefficient of smoothness

*** n.s. ***

R:N R:R RScb:N REphA2 KD:N

G GFP-RasV12 | EphA2 | F-actin

Scramb shRNA

EphA2 shRNA-1

H Nuclei / GFP-RasV12 | EphA2 | F-actin

Scramb shRNA

GFP-RasV12 Normal

EphA2 shRNA-1

GFP-RasV12 Normal

I

% apically extruded GFP-RasV12 cells

**

Scramb shRNA EphA2 shRNA-1 EphA2 shRNA-2

A GFP-RasV12 cells | Normal cells
GFP/Nuclei/Fc | F-actin/Nuclei/Fc
Fc
Ephrin-A1-Fc
Ephrin-A4-Fc

B Scramb shRNA | EphA2 shRNA-1
GFP/Fc
Fc
EphrinA1-Fc
EphrinA4-Fc

C GFP-RasV12 | E-cadherin
Fc
Ephrin-A1-Fc
Ephrin-A4-Fc

D Nuclei / GFP-RasV12 | EphA2 | F-actin
Untreated
Scramb shRNA | + Fc
+ EphrinA1-Fc
EphA2 shRNA-1 | + Fc
+ EphrinA1-Fc

E Normal cells
+PBS | +PI-PLC
WB: anti-EphrinA1
WB: anti-GAPDH

F Nuclei / GFP-RasV12 | EphA2 | pEphA2
+ PBS
+ PI-PLC

G
IND (μm)
***
Untreated control | + PBS | + PI-PLC

A Nuclei/GFP · EphA2 · CMRA dye

Scramb shRNA · RasV12

EphA2 shRNA-1 · RasV12

B Cell Area (μm²)

Ras: Scramble · Ras: EphA2 KD

***

C IND (μm)

Ras:Scramble · Ras:EphA2 KD

***

D XY

GFP only · GFP + RasV12

Nuclei/GFP

Fc

E XZ

GFP only · GFP + RasV12

Nuclei/GFP · Apical · Basal

Fc · Apical · Basal

F XY

GFP + RasV12 + RNAi GD2535 + KK101831

GFP + RasV12 + DEph DN

Nuclei/GFP

Fc

G XZ

Nuclei/GFP · Apical · Basal

Fc · Apical · Basal

A
1: Cell seeding +8-16h 2: Remove culture insert 3: Add culture media

B
0' +100' +130' +160' +190'
GFP-RasV12
R:N
Merge

C
Merge Cell tracks
N:R
R:R

D
Cell Area (μm²)
R:N
R:R
REphA2 KD:N
RScb:N
*** ** ***
Cell rows from collision interface
1 2-5 6-10 11 +

E
GFP F-actin
RasV12 Normal t = 19 h
RasV12 Normal t = 48 h
RasV12 RasV12 t = 48 h
Normal Normal t = 48 h
Ras + EphA2 shRNA-1 Normal t = 48 h

F
GFP F-actin EphA2
R:N -2 h
+7 h
+23 h

G
Cell Area (μm²)
DMSO PP2 Blebb. U0126
***

H
Y27632
Blebb.
ML-7
U0126 *
PP2 *
DMSO
Distance (μm)
-250 -200 -150 -100 -50 0

I
GFP pMLC F-actin
R:N
R:R

A

1: No cDNA control
2: Normal
3: GFP-RasV12 (+ Tet)

1   2   3

EphA1

EphA2

EphA3

ephrin-A1

ephrin-A4

Actin

B

	Normal	GFP-RasV12		
Tet (24h)	–	–	+	+
U0126	–	–	–	+

WB: anti-EphA2

WB: anti-GFP

WB: anti-GAPDH

C

+ ephrin-A5-Fc
+ ephrin-A4-Fc   *
+ ephrin-A3-Fc
+ ephrin-A1-Fc   **
+ ephrin-B3-Fc
+ ephrin-B2-Fc
+ ephrin-B1-Fc
+ Fc

-250   -200   -150   -100   -50   0

Distance (μm)

D

Cell Area (μm²)

400
300
200
100

***

+ Fc   + ephrin-A1-Fc   + ephrin-A4-Fc

E

GFP-RasV12	EphA2	Merge

+ Fc

+ephn-A1-Fc

+ephn-A4-Fc

F

N   RasV12

WB: anti-Ephrin A1

WB: anti-GAPDH

G

Relative density

1.5
1.0
0.5

■ Ephrin A1 lysates
□ Ephrin A1 beads

Normal   RasV12
only   only

A

GFP-RasV12 | EphA2 | pEphA2

R:N
1:100

RasV12
cells only

B

Fold increase in phosphorylated EphA2 intensity

n.s.

*** ***

N:N   R:N   R:R

RasV12:Normal cells, 1:100

C

+ Tet (24h)

RasV12 +

N | RasV12 | KD-1 | KD-2 | Scb

WB: anti-EphA2

WB: anti-GAPDH

D

Nuclei /
GFP-RasV12 | EphA2 | pSrc

Scramb
shRNA

EphA2
shRNA-1

E

GFP-RasV12 | EphA2 | pSrc

GFP-RasV12
cells only

F

GFP-RasV12:Normal, 1:100

RasV12 +
Scb shRNA | RasV12 +
EphA2 shRNA-1 | RasV12
cells only

Nuclei/
GFP-RasV12

EphA2

pEphA2

RasV12 +
Scb shRNA | RasV12 +
EphA2 shRNA-1 | RasV12
cells only

Nuclei/
GFP-RasV12

EphA2

pSrc

G

GFP | pMLC | F-actin

Ras + Normal
EphA2
shRNA-1

A

B ptc-Gal4 UAS-GFP   Eph:V5

GD2535

KK101831

C GFP + RasV12
+
RNAi GD2535 + KK101831

Nuclei/GFP

Nuclei

Fc

D

E 1. Cell-cell interaction

EphA2 ephrin-A

2. RasV12 cell repulsion, contractility

pEphA2
pSrc

actin-myosin
cytoskeleton

3. RasV12 cell-cell contractility

pEphA2

RasV12 cells

Normal cells

EphA2 protein

pEphA2 protein

Figure S1. Upon collision with normal cells, RasV12 cells display cell repulsion and increase actin-myosin contractility. Related to Figure 1 and Figure 2.
(**A**) Cartoon illustrating the cell confrontation assay. (**B**) Epifluorescence (top panels) and merged bright field images (lower panels) extracted from a representative time-lapse experiment of a cell confrontation assay of non-labelled normal cells colliding with GFP-RasV12 cells. Elapsed time is indicated minutes after collision. White arrowhead indicates GFP-RasV12 lamellipod. (**C**) Representative single cell analyses of cell migration. Tracked GFP-RasV12 cells are indicated on the merged images (left panels). Right panels show single cell tracks over a 15 h time period post collision with opposing cells in cell confrontation assays. Top panels: normal cells confronting GFP-RasV12 cells (N:R); Lower panels: GFP-RasV12 cells confronting GFP-RasV12 cells (R:R). (**D**) Quantification of GFP-RasV12 cell area (μm^2) from each of the first ten rows of cells and behind row 11 (11+) from the collision interface using the cell confrontation assay. The number of rows available for quantification in rows 11+ varied between experiments and was determined by field of view (up to row 14). A minimum of 14 cells were analysed per subset of rows. Black bars: GFP-RasV12 cells colliding with normal cells (R:N, n = 465 total cells); White bars: GFP-RasV12 cells colliding with GFP-RasV12 cells (R:R, n = 150 total cells); Grey bars: GFP-RasV12 cells constitutively expressing EphA2 shRNA-1 colliding with normal cells (REphA2 KD:N, n = 327 total cells); Blue bars: GFP-RasV12 cells constitutively expressing scramble shRNA colliding with normal cells (RScb:N, n = 500 total cells). Data represents mean ± s.e.m. from three independent experiments; *** $p < 0.001$; ** $p < 0.01$ for R:N versus R:R and RScb:N versus REphA2 KD:N. (**E**) Confocal images of cell confrontation assays of GFP-RasV12 cells colliding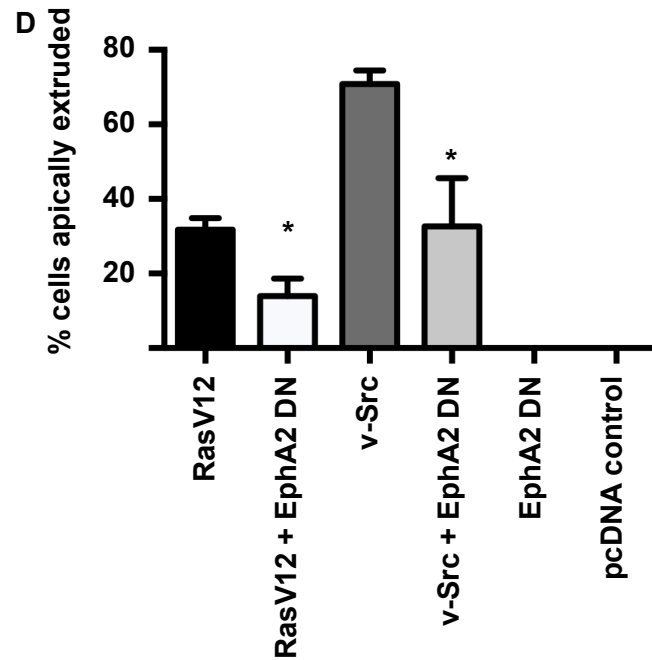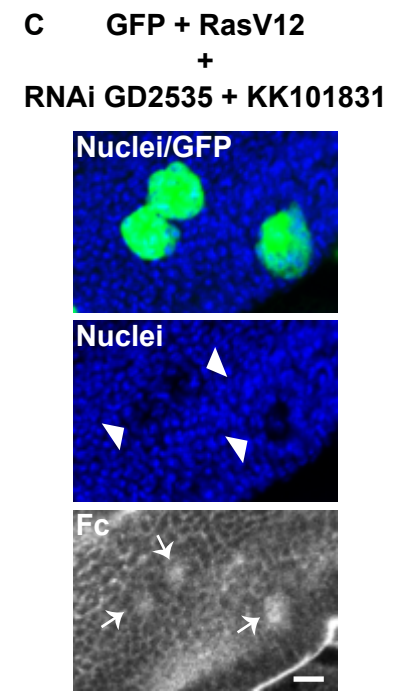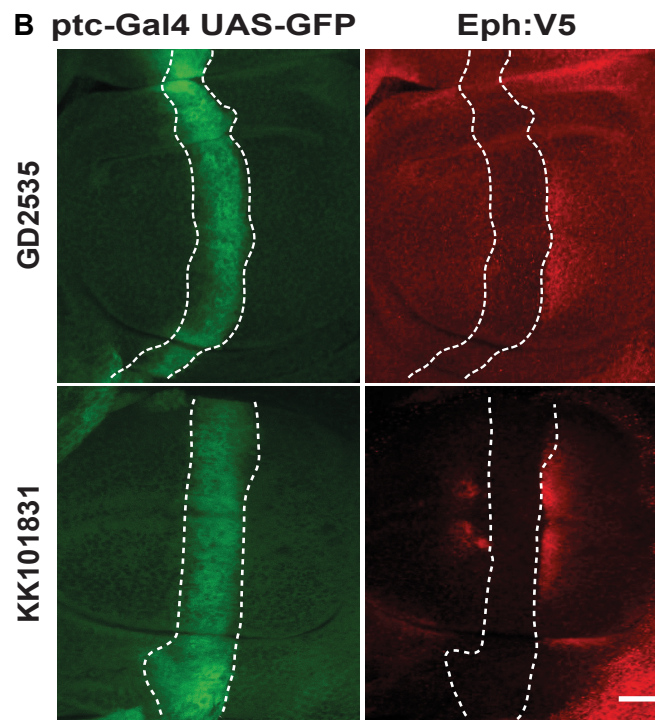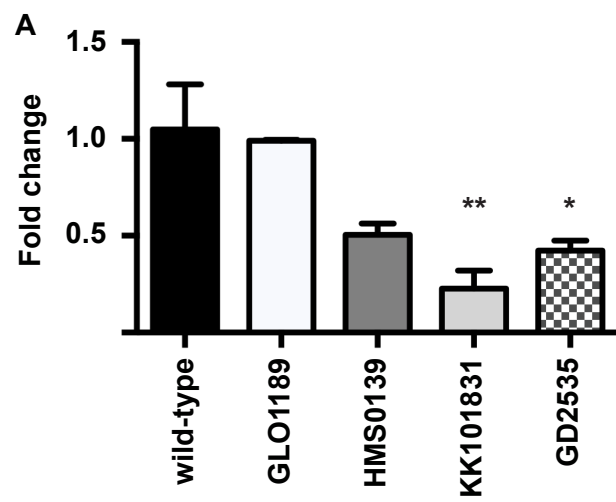 with normal cells (upper panels), GFP-RasV12 cells colliding with GFP-RasV12 cells (middle panels), GFP-labelled normal cells colliding with normal cells (lower panels), or GFP-RasV12 cells expressing shRNA-1 colliding with normal cells (bottom panels). Cells were fixed at 19 h (top panels only; ~1-2 h pre-collision) or 48 h following addition of tetracycline (~24 h post collision). Fixed cells were stained with phalloidin (red). Images are maximum projections of z stacks. (**F**) Confocal images of cell confrontation assays of GFP-RasV12 cells colliding with normal cells (R:N). Cells were fixed at 19 h (~2 h pre collision), 29 h (~7 h post collision), and 45 h (~23 h post collision) and stained with phalloidin (red) and anti-EphA2 (grey). Images are maximum projections of z stacks. (**G**) Quantification of GFP-RasV12 cell area (μm^2) in cell confrontation assays with normal cells in the presence of various inhibitors. White bar: DMSO (n = 363 cells); Black bar: PP2 (SFK inhibitor; n = 279 cells); Grey bar: Blebbistatin (myosin-II inhibitor; n = 503 cells); Light grey bar: U0126 (MEK/ERK inhibitor; n = 305 cells). Data represent mean ± s.e.m from three independent experiments; *** $p < 0.001$. (**H**) Quantification of distance (μm) travelled by marginal GFP-RasV12 cells following collision with normal cells until the end of the experiment (42 h) in the presence of various small molecule inhibitors. White bar: DMSO; Black bar: PP2; Light grey bar: U0126; Hatched grey bar: ML-7 (Myosin light chain kinase inhibitor; Dark grey bar: Blebbistatin; Striped bar: Y27632 (ROCK inhibitor). Data indicate mean ± standard deviation (s.d.) from at least three independent experiments; * $p < 0.05$ for DMSO versus PP2, U0126. (**I**) Confocal images of cell confrontation assays. Upper panels: GFP-RasV12 cell sheets confronting normal cells (R:N); Lower panels: GFP-RasV12 cells confronting GFP-RasV12 cells (R:R). Cells were fixed 41 h after addition of doxycycline (~17-19 h post collision) and stained with anti-phosphorylated myosin light chain (pMLC; grey) and phalloidin (red). Images are maximum projections of z stacks. Scale bar, 20 μm (**E**, **F**, **I**). Scale bar, 50 μm (**B-C**).

Figure S2. Exploring the functional role of EphA2 in GFP-RasV12 cell clustering and segregation. Related to Figure 2 and Figure 4.

(**A**) RT-PCR analyses of EphA1, EphA2, EphA3, ephrin-A1 and ephrin-A4 mRNA from normal MDCK (lane 2) or GFP-RasV12 cells (lane 3) treated with tetracycline for 16 h (+Tet). Expression of actin mRNA from both cell lines was included as positive control (bottom panel). PCR reaction in the absence of cDNA template was included as negative control (lane 1). (**B**) Tetracycline-induced expression of GFP-RasV12 and EphA2 protein in MDCK cell lines as determined by Western blotting using anti-GFP and anti-EphA2 antibodies, respectively. Lysates were isolated from cells following 24 h of tetracycline induction, and in the presence or absence of the MEK/ERK inhibitor U0126 for 24 h. GAPDH protein was detected using anti-GAPDH antibodies and included as loading control. (**C**) Quantification of distance (μm) travelled by marginal GFP-RasV12 cells in cell confrontation assays with normal cells (not depicted). Assays were performed in the presence of 2 μg ml^{-1} soluble recombinant Fc (white bar), ephrin-B-Fc (blue bars) or ephrin-A-Fc (grey bars) proteins. Distance was measured from collision with normal cells until the end of the experiment (42 h). Data indicate mean ± s.e.m. from a minimum of three independent experiments; ** $p = 0.005$; * $p < 0.05$ for Fc versus all other conditions. Addition of ephrin-B-Fc ligands yielded no significant difference compared to Fc controls. (**D**) Quantification of RasV12 cell area (μm^2) in cell confrontation assays with normal cells in the presence of soluble recombinant Fc proteins. White bar: + Fc (n = 828 cells); Black bar: + ephrin-A1-Fc (n = 534 cells); Grey bar: + ephrin-A4-Fc (n = 317 cells). Data represent mean ± s.e.m. from three independent experiments; *** $p < 0.001$. (**E**) Confocal images of cell confrontation assays of GFP-RasV12 cells confronting normal (non-labelled) MDCK cells. Assays were performed in the presence of 2 μg ml^{-1} soluble recombinant Fc protein (upper panels), ephrin-A1-Fc (middle panels), or ephrin-A4-Fc (lower panels). Cells were fixed at 24 h post collision and stained with anti-EphA2 antibody (grey). Dashed white line depicts border between GFP-RasV12 and normal cells. (**F**) Western blot of total cell lysates isolated from normal (N) or GFP-RasV12 cell lines (RasV12), 24 h after addition of doxycycline. Expression of ephrin-A1 or GAPDH was detected using anti-ephrin-A1 (top panels) and anti-GAPDH (lower panels), respectively. (**G**) Quantification of ephrin-A1 levels expressed on the cell surface of normal or RasV12 cells (beads, white bars) relative to total ephrin-A1 protein levels (lysates, black bars) as determined by biotinylation and Western blotting assays (n = 5). Data comparing the relative level of ephrin-A1 between normal and RasV12 cells are not significant. Scale bar, 20 μm (**E**).

Figure S3. Functional role of EphA2 and downstream signalling pathways in RasV12-normal cell-cell interactions. Related to Figure 2.

(**A**) Confocal images of GFP-RasV12 cells mixed with normal MDCK cells at 1:100 ratios (upper panels) and GFP-RasV12 monolayers (lower panels). Cells were fixed 48 h after addition of doxycycline and stained with anti-EphA2 (grey) or anti-phospho-EphA2 (pEphA2, Y594; cyan) antibodies. (**B**) Quantification of fold increase in phosphorylated EphA2 intensity detected at cell-cell contacts between normal cells (N:N: dark blue bar, n = 90 measurements); GFP-RasV12 and normal cells (R:N: light blue bar, n = 42 measurements); GFP-RasV12 cells within a cluster and surrounded by normal cells (R:R: patterned blue bar, n = 60 measurements). Data represent mean ± s.e.m. from three independent experiments; *** $p < 0.001$ for

comparisons between N:N and R:N, or N:N and R:R. Comparisons between R:N and R:R were not significant (n.s.). (**C**) Expression levels of EphA2 protein in MDCK cell lines in the presence of tetracycline (+ Tet) for 24 h. Cell lysates were examined from normal MDCK (N), MDCK-pTR-GFP-RasV12 (RasV12), MDCK-pTR-GFP-RasV12 constitutively expressing either EphA2 shRNA-1 or shRNA-2 (KD-1 or KD-2) or scramble shRNA (Scb) by Western blotting using the indicated antibodies. (**D**) Confocal images of MDCK-pTR-GFP-RasV12 cells constitutively expressing either scramble shRNA (upper panels) or EphA2 shRNA-1 (lower panels) mixed with normal MDCK cells at 1:100 ratios. Cells were fixed 48 h after addition of doxycycline, and stained with anti-EphA2 (grey) or anti-phosphorylated Src (pSrc, Y416; magenta) antibodies and Hoechst (blue). (**E**) Confocal images of a monolayer of GFP-RasV12 cells fixed 48 h after addition of doxycycline and stained with anti-EphA2 (grey) or anti-phosphorylated Src (pSrc, Y416; magenta) antibodies. (**F**) XZ orthogonal views of z-stacks as in (D) (left, central panels) or of GFP-RasV12 monolayers (RasV12 cells only; right panels), stained with anti-EphA2 (grey) and either anti-phospho-EphA2 (pEphA2, Y594; cyan) or anti-phosphorylated Src (pSrc, Y416; magenta) antibodies and Hoechst (blue). (**G**) Confocal images of cell confrontation assays of GFP-RasV12 cells expressing EphA2 shRNA-1 confronting normal cells (Ras+EphA2 shRNA-1:Normal). Cells were fixed 41 h after addition of doxycycline (~17-19 h post collision) and stained with anti-phosphorylated myosin light chain (pMLC; grey) and phalloidin (red). Images are maximum projections of z stacks. Scale bar, 20 μm (**A, D-G**).

Figure S4. Elevated expression of Eph receptors are functionally required to promote transformed cell extrusion in vitro and in vivo. Related to Figure 4.
(**A**) Quantification of fold change in *Drosophila* DEph expression at the mRNA level in imaginal discs isolated from transgenic flies expressing one of four RNAi constructs (GLO1189, HMS0139, KK101831, GD2535) compared to wild-type. Data represent means ± s.d., n = 3 technical replicates on RNA pooled from several individual larvae. ** $p < 0.01$, * $p < 0.05$ for wild-type levels versus expression of RNAi. All other comparisons were not significant. (**B**) Confocal images of *Drosophila* wing imaginal discs expressing *UAS-GFP* (green, left panels) and either *UAS-DEph*[RNAi]*-GD2535* (upper panel) or *UAS-DEph*[RNAi]*-KK101831* (lower panel), stained for DEph protein expression using an endogenously tagged *DEph:V5* transgene (red, right panels). Area within the broken white lines shows that expression of each RNAi construct induced a reduction in DEph staining. Posterior is to the right and dorsal to the top. (**C**) Confocal images of *Drosophila* wing imaginal discs harbouring clones co-expressing GFP and RasV12 and two RNAi constructs (GD2535, KK101831). Epithelial tissues were incubated with soluble Dephrin-Fc protein before being fixed and stained with anti-Fc antibody (grey) and Hoecht (blue). White arrowheads indicate rearrangement of nuclei indicative of cyst-like clusters. White arrows indicate Dephrin-Fc staining in contractile RasV12 cells, indicating incomplete knockdown of DEph. (**D**) Quantification of apical extrusion of normal cells seeded on collagen gels and transiently transfected with DNA constructs. Black bar: GFP-RasV12 and pcDNA (n = 355 cells); White bar: GFP-RasV12 and HA-tagged EphA2 deltaC (+EphA2 DN; n = 362 cells); Dark grey bar: GFP-tagged v-Src (Src Y576F) and pcDNA (n = 238 cells); Light grey bar: GFP-tagged v-Src and HA-tagged EphA2 deltaC (+EphA2 DN; n = 226 cells). Co-expression of HA-tagged EphA2 deltaC (EphA2 DN) and GFP, or pcDNA vector and GFP (pcDNA control) did not induce apical extrusion of cells. Cells were fixed 24 h after transfection. Data

represent mean ± s.e.m. from three independent experiments, except HA + GFP (pcDNA control), n = two experiments. * p < 0.05 for comparisons between v-Src versus v-Src + EphA2 DN and RasV12 versus RasV12 + EphA2 DN. (**E**) Model showing that (1) cell-cell interactions between sheets of RasV12 (green) and normal epithelial cells triggers EphA2-ephrin-A signals at the RasV12:Normal cell-cell interface. (2) This activates EphA2 receptor (pEphA2) expressed on RasV12 cells and SFK (pSrc) to modulate RasV12 cell shape and myosin-II-dependent contractility. Subsequently, (3) neighbouring RasV12 cells that are positioned behind marginal cells and not in direct contact with normal cells are triggered to contract in an EphA2-dependent manner. A combination of the initial repulsion signal and the concomitant contractility, promotes the segregation of RasV12 cells from normal cells. Scale bar, 20 μm (**B-C**).

Supplemental Movies S1; Related to **Figure 1** and **Figure S1**.
Representative time-lapse experiment of cell confrontation assays of non-labelled normal cells colliding with GFP-RasV12 cells as depicted in Figure 1A (left panels). Movie is a composite of bright field images and fluorescence images captured at 488 nm (GFP). Duration is 30 h.

Supplemental Movies S2; Related to **Figure 1** and **Figure S1**.
Representative time-lapse experiment of cell confrontation assays of GFP-RasV12 cells colliding with GFP-RasV12 cells as depicted in Figure 1A (right panels). Movie is a composite of bright field images and fluorescence images captured at 488 nm (GFP) and 568 nm (CMTPX tracker dye), which are shown every 10 h. Duration is 30 h.

Supplemental Movies S3; Related to **Figure 1** and **Figure S1**.
Combined movies of individual trajectories of 10 cells tracked post-collision in cell confrontation assays. Movie on the left shows GFP-RasV12 cells colliding with GFP-RasV12 cells, as depicted in Figure S1C (lower panels). One population of GFP-RasV12 cells was prestained with cell tracker dye in order to demarcate the collision interface. Movie on the right shows non-labelled normal cells colliding with GFP-RasV12 cells, as depicted in Figure S1C (upper panels). Numbered end of track indicates direction of cell movement. Cells were tracked over 15 h.

Supplemental Movies S4; Related to **Figure 1** and **Figure S1**.
Representative time-lapse experiment of cell confrontation assays of non-labelled normal cells (left) colliding with non-labelled RasV12 cells (right) in the presence of blebbistatin (25μM). Fluorescence images were not captured, as blebbistatin is blue light sensitive. Inhibitor was added approximately 30 min prior to recording. Duration is 30 h.

Supplemental materials and methods

Antibodies, Plasmids and Reagents

Primary antibodies used: Rat anti-E-cadherin (ECCD2) (Life technologies); rabbit anti-phospho-EphA2 (Y594) (p-EphA2), rabbit anti-phospho-Src (Y416) (p-Src), rabbit anti-phospho-myosin light chain (pMLC), all from Cell Signaling Technology; anti-GAPDH (Chemicon International); mouse anti-EphA2 (clone D7) (Millipore) or rabbit anti-EphA2 (Santa-Cruz); rabbit anti-ephrin-A1 (Abcam); mouse anti-GFP (Roche). Secondary antibodies (Alexa-405-, Alexa-568-, Alexa-546- and Alexa-647-conjugated anti-rat, anti-mouse and anti-rabbit) were from Life Technologies. DNA plasmids used include: pcDNA3.1-HA (kindly provided by M. Razi, The Francis Crick Institute, London), pShuttle-HA-EphA2 deltaC (generously provided by N. Mochizuki, National Cerebral and Cardiovascular Center Research Institute, Japan), pcDNA4/T0/GFP-SrcY574F and pcDNA4/T0/GFP were constructed as previously described SS1, S2]. (S)-(-)-blebbistatin (Tocris Bioscience) was used at 25 μM; U0126 from Promega was used at 10 μM; PP2, ML-7 and Y27632 were from Millipore (Calbiochem) and were used at 10 μM. All inhibitors were added to cell confrontation assays at collision, or ~1 h prior to collision until the end of the experiment (42 h). DMSO (Sigma-Aldrich) was added at a dilution of 1:1,000 as control.

Cell culture and RNA interference

Normal MDCK cells, MDCK-pTR cell lines stably expressing GFP-RasV12 in a Tet-ON inducible manner or E-cadherin shRNA were cultured as previously described [S1]. MDCK-pTR-GFP-RasV12 cell lines constitutively expressing EphA2 shRNA were produced using EphA2 shRNA oligonucleotides (EphA2 shRNA-1: 5'-GATCCCCGTCTAACAGGGACAAAGAATTCAAAGAGATTCTTTGTCCCTGTTAGACTTTTTC-3'; EphA2 shRNA-2: 5'-GATCCCCGCAGCAAGATTCACGAGTTTTCAAGAGAAACTCGTGAATCTTGCTGCTTTTTC-3'). Scramble shRNA oligonucleotides were designed as previously described [S3]. EphA2 or scramble shRNA were cloned into BglI and XhoI sites of pSUPER.neo+gfp (Oligoengine, Seattle, WA). MDCK-pTR-GFP-RasV12 cells were transfected with pSUPER.neo+gfp EphA2 or scramble shRNA using Lipofectamine 2000 (Life Technologies), followed by selection in medium containing 800 μg ml^{-1} of G418 (Calbiochem). More than two stable clones were obtained for two independent shRNA oligonucleotides. Depletion of EphA2 was analysed by immunofluorescence and Western blotting following 24 h incubation with tetracycline or doxycycline (2 μg ml^{-1}). Comparable effect of EphA2 depletion on segregation, cell repulsion or apical extrusion was observed in cells expressing EphA2 shRNA-1 or -2. Cells were plated as described below, except where indicated as low-density; cells were plated at 1 x 10^3 cells in 4-well culture dishes (Nunc, Roskilde, Denmark).

Coculture assays, Cell confrontation assays and Time-lapse microscopy

MDCK-pTR-GFP-RasV12 cells were trypsinised and mixed with non-labelled normal MDCK cells at a ratio of 1:100. Cells were plated at a density of 4 x 10^5 on 13 mm serum-coated glass coverslips. Mixed cells were incubated for 8-16 h at 37°C before being switched to tetracycline/doxycycline-containing medium. Cell confrontation assays were set up using commercially available cell culture inserts (Ibidi GmbH) according to manufacturer's instructions. Briefly, MDCK-pTR-GFP-RasV12, MDCK-pTR-GFP, or normal MDCK cells were seeded into one of two compartments, at a density of 3-4 x 10^4 cells. Cells were incubated for 8-16 h at 37°C before removal of the culture insert and switched to tetracycline/doxycycline-containing medium. Cell sheets were allowed to collide before addition of inhibitors or unclustered Fc proteins. In order to monitor cell morphology changes over time, we fixed cells at different time points post collision. Generally, we observed repulsion of RasV12 cells in the first 5 rows from the cell margin at 30-40 h (e.g., Figure 1D, 1G), and repulsion of RasV12 cells beyond rows 1-5 at 48 h (e.g., Figure S1E) post treatment with tetracycline/doxycycline. In order to capture differences in RasV12 cell morphology; e.g., in marginal cells

immediately post collision, or in the cell sheet at later time points, we monitored cells over time and fixed cells when RasV12 cell changes were observed. To obtain time-lapse images, we used a Zeiss Axiovert 200M microscope with a Ludl Electronic Products Biopoint Controller and a Hamamatsu C4742-95 Orca camera (Hamamatsu) or a Leica automated inverted DMI6000B microscope system with Leica DFC365FX camera. Images were captured using Volocity (Improvision) or Leica Application Suite (LAS) image analysis software (v3.2.0). Data in Figure 1B, S1G were analysed using Metamorph 6.0 digital analysis software (Universal Imaging), and in Figure 2D, S2C using LAS (Leica) image analysis software. Single-cell tracking of cells in the confrontation assay was performed using the manual tracking plugin in Fiji (National Institute of Health) (v1.48j) software. Cells in rows 1-5 and rows 5-10 were demarcated at collision and their subsequent positions were manually recorded every 10 frames (100 minutes) for 15 h post-collision.

Collagen assays

To quantify apical extrusion, co-culture experiments were carried out on type I collagen gels (Nitta Gelatin) as previously described [S1]. Briefly, cells were plated at a total of 1×10^6 cells per 35-mm well where GFP-RasV12 cells were mixed with normal cells at ratios of 1:100. Cells were incubated for 8-16 h at 37°C before inducing GFP-RasV12 expression with tetracycline/doxycycline. Cells were fixed 24 h later and stained as previously described [S1].

For transient expression experiments, normal MDCK cells were first seeded on collagen I gels at a density of 7×10^5 per 35-mm well. On the following day, cells were transiently transfected with the indicated DNA constructs using Lipofectamine™ 3000 according to manufacturer's instructions (at 2 μg per construct). Cells were fixed at the indicated time points and stained as previously described [S1]. Apical extrusion was scored as previously described [S1]. Briefly, apical extrusion was scored when single or small clusters of cells (3-5 cells) were eliminated from the apical side of the epithelial cell sheet.

Recombinant Fc- protein treatment of cell lines

Recombinant ephrin-A-Fc or ephrin-B-Fc ligands were from R&D systems and recombinant Fc proteins from Millipore. For inhibition of Eph-ephrin signalling experiments, unclustered ephrin-A-Fc, ephrin-B-Fc or Fc proteins were added to cell confrontation assays at cell collision at 2 μg ml^{-1}. Recombinant ephrin-A1-Fc or ephrin-A4-Fc fusion proteins were pre-clustered with anti-human Fc antibodies at a 2:1 molar ratio and added to MDCK-pTR-GFP-RasV12 cells, or MDCK-pTR-GFP-RasV12 cells expressing EphA2 (or scramble) shRNA at a final concentration of 10 μg ml^{-1}. Cells were incubated for 24 h before fixing. For modified stripe assays, pre-clustered ephrin-A1-Fc, ephrin-A4 or Fc proteins (10 μg ml^{-1}) were added to one compartment of the culture insert used in cell confrontation assays. Stripes of pre-clustered Fc proteins were incubated at 37°C for 30 min and washed once with PBS. Fc stripes were visualised with anti-Fc antibodies (Jackson labs) and fluorescence. Normal MDCK, MDCK-pTR-GFP-RasV12 cell lines or MDCK-pTR-GFP-RasV12 cells constitutively expressing EphA2 shRNA or scramble shRNA, were seeded in the second compartment. Cells were incubated for 8-16 h at 37°C before removal of the culture insert and switched to tetracycline/doxycycline-containing medium. All RasV12 cell lines were fixed and analysed 72 h later. Normal cells were fixed and analysed at 96 h.

Immunofluorescence

Immunofluorescence of cells cultured on serum-coated glass coverslips was performed as previously described [S4], except for experiments using anti-phospho-specific antibodies; here the protocol was modified to include 1X TBS with 1 mM NaF, 1 mM Na$_3$VO$_4$ in all washing and blocking steps. All primary antibodies were used at a dilution of 1:100 except p-EphA2 (Y594), p-MLC and p-Src (Y416) antibodies, which were used at 1:50. All secondary antibodies were used at 1:200-1:400 dilutions. TRITC-phalloidin (Sigma-Aldrich) was used at 1.5 μg ml^{-1}. In some experiments, GFP-RasV12 cells were prestained with a cell tracker dye as previously described [S1] (Red: CMTPX or Orange: CMRA; both from Life

Technologies). Cells cultured on glass coverslips were examined using either a Leica TCS SPE confocal microscope, Leica DMI600B inverted epifluorescence microscope with a Leica DFC365FX camera, or Zeiss LSM710 confocal microscope. Images were analysed using LAS software (v3.2.0), Zen (Zeiss Efficient Navigation) software, or Fiji (National Institute of Health) (v1.48j) software.

Quantitative image analysis

Inter-nuclear distance (IND) was calculated by measuring the distance between the centre of nuclei of neighbouring cells in direct contact in GFP-labelled cell clusters in 1:100 co-culture assays. Measurements were made by first using point-picker in Fiji (v1.48j) to demarcate the centre points of nuclei, followed by Voronoi analysis using custom scripts in Python (v3.3) to measure the distance between these centre points from a minimum of three repeated experiments. To analyse the cell area in confrontation assays, single z-stack slices were converted to 8-bit grayscale images in Fiji (v1.48j) and segmented using Packing Analyzer (v2.0) [S8]. The flood area feature in Packing Analyzer was used to give total cell areas in pixels, which were then converted to areas in μm^2 using metadata. Cells in the y-axis in direct contact with the opposing cell sheet were demarcated as row 1 and subsequent cells behind as row 2, row 3 etc. based on their position in the x-axis relative to row 1 cells. The number of rows available for quantification in rows 11+ varied between confrontation assays and was determined by field of view but generally extended to row 14. A minimum of 14 cells were analysed per subset of rows. To measure the coefficient of boundary smoothness between interacting cell sheets in the cell confrontation assay, we performed analysis as previously described [S5].

PI-PLC treatment, Biotinylation assays and Immunoblotting

Endogenous ephrin-A ligands were cleaved from the cell surface of normal cells as previously described [S6]. Briefly, cells were pre-treated with 1 U ml^{-1} PI-PLC (Life Technologies), or an equivalent volume of PBS for 4 h before being switched back to regular DMEM/FCS media. Untreated controls were also included. Cells were then trypsinised and used in 1:100 co-culture assays. Cell lysates were also harvested at 4 h or 28 h post-treatment.

To detect ephrin-A1 expressed at the cell surface of normal or GFP-RasV12 cell lines, we performed biotinylation assays as previously described [S7]. Briefly, sub-confluent MDCK cells were placed on ice and washed twice in ice cold PBS. Cells were then incubated with 1 mg ml^{-1} EZ-link SulfoNHS-SS-biotin (Pierce/Thermo Scientific) in PBS for 30 min at 4°C followed by one wash with cold PBS and incubation in quenching buffer (50 mM NH$_4$Cl in PBS containing 1 mM MgCl$_2$ and 0.1 mM CaCl$_2$) for 5 min at 4°C. The cells were then lysed in RIPA buffer (20 mM Tris-HCl pH 7.4, with 150 mM NaCl, 0.1% SDS, 1% Triton X-100, 1% deoxycholate, 5 mM EDTA) plus protease inhibitors. Lysates were centrifuged to obtain a detergent-soluble supernatant, which was incubated with streptavidin (Neutravidin) beads (Pierce/Thermo Scientific) for 1 h, rotating at 4°C to collect bound, biotinylated proteins. Samples were then analyzed by SDS-PAGE and immunoblotting to identify ephrin-A1. Immunoblotting analyses were performed using the following antibodies: rabbit anti-EphA2 (Santa Cruz), mouse anti-GFP (Roche) at 1:1,000, mouse anti-GAPDH (Chemicon International) at 1:5,000, rabbit anti-ephrin-A1 (Abcam) at 1:500. Secondary HRP-conjugated antibodies were from Sigma; ECL reagent from Pierce. Immunoblots were developed and band intensity quantified using a Biorad Gel-doc system.

Expression and purification of recombinant Fc proteins

pCEP4 Dephrin-Fc and pCEP4 Fc plasmids were kindly provided by Philip F. Copenhaver (Oregon Health & Science University). HEK293 cells (grown in DMEM, 10% FCS, 1% penicillin/streptomycin, 1% glutamax) were seeded in 15-cm dishes and allowed to reach 70% confluence, before being transfected with pCEP4 plasmids using Lipofectamine 3000 (Life technologies). The next day, cells were switched to serum-free media (DMEM plus 1% penicillin/streptomycin, 1% glutamax), and cultured for 6 days. Protein was purified as previously described [S8, S9]. Briefly, the pH of the conditioned media was adjusted to pH 8.0

before incubating with protein A sepharose beads (Sigma) and collected using affinity chromatography (Pierce). Beads were washed three times with 100 mM Tris Cl, pH 8.0, followed by elution using 100 mM glycine, pH 3.0 and collected into 1 M Tris Cl, pH 8.0. Pooled fractions were dialyzed against sterile PBS (pH 7.4) and stored at 4°C. Fc protein integrity was assessed by coomassie blue staining of polyacrylamide gels and concentrations were determined using Nanodrop spectroscopy. We were unable to purify adequate quantities of Fc protein using this method; therefore commercial Fc protein was used as a control in experiments using *Drosophila* wing imaginal discs.

Generation and analyses of GFP and RasV12 overexpressing clones in *Drosophila melanogaster* wing imaginal discs

Drosophila larvae were reared on standard cornmeal medium, at 25°C unless otherwise indicated. GFP-labelled clones were induced 72-96 h after egg laying (AEL) by heat treatment at 35°C for 10 min, and wing imaginal discs were dissected two days later. Experimental larvae were obtained by crossing *hs-FLP1.22; Act5C-FRT-y[+]-FRT-Gal4, UAS-GFP* flies with *UAS-Ras^{V12}*, or *UAS-Dcr2; UAS-Ras^{V12}, UAS-DEph^{RNAi}KK101831; UAS-DEph^{RNAi}GD2535* [S10], or *UAS-Ras^{V12}; UAS-DEph^{DN}* flies [S11]. DEph receptor was detected using purified Dephrin-Fc, as previously described [S6]. Fc proteins were detected using goat anti-human Fc (Sigma). To test the relative efficiency of different RNAi constructs, first we raised *hs-FLP1.22; UAS-DEph^{RNAi} / UAS-GFP; Act5C-FRT-y[+]-FRT-Gal4SwitchPR* flies, induced ubiquitous recombination by heat shock treatment (60 min at 37°C) at 72-96 h AEL and immediately afterwards, Mifepristone was added (Sigma, 500μg per vial) to activate the Gal4SwitchPR transcriptional regulator. Total RNA was extracted from larvae two days later, on which qRT-PCR analysis was performed using the primers 5'-TGGAACTGGTCAAATCAGGACGTG-3' and 5'-ATCCATCGGAGCTGGTAAACGG-3' with SYBR Green Master Mix reagent on a QuantStudio 7 Flex instrument (Life Technologies). We then raised *UAS-Dcr2; ptc-Gal4, UAS-GFP / UAS-DEph^{RNAi}; DEph:V5* (*DEph:V5* is a transgene from the fly-TransgeneOme collection, inserted on the 3rd chromosome, comprising the full genomic region of the *DEph* gene, and tagged with 2XTY1-SGFP-V5-preTEV-BLRP-3XFLAG [S12]) flies at 29°C and tested each RNAi for *DEph* expression in the wing pouch of 3rd instar larvae with anti-V5 (R960-25, Invitrogen). Secondary antibodies were donkey anti-goat and goat anti-mouse conjugated to Alexa568 (Life Technologies). Discs were examined and imaged using a Zeiss LSM710 confocal microscope; images were analysed using Fiji (v1.48j). Segregating clones were scored in the wing pouch only, consistent with our previous study [S1].

Statistical analyses

All data were plotted in Prism 6 (Graphpad). Error bars on graphs represent mean ± standard error of the mean (s.e.m.) except for Figure 1B, Figure S1G and Figure S2C; here error bars on graphs represent mean ± standard deviation of the mean (s.d.). To test for statistical significance between experimental groups, one-way ANOVAs were performed with a Dunn's post-hoc test; except for time-lapse data depicted in Figure 1B and data comparing differences in cell area, which were analysed using two-tailed parametric t-tests (with or without Welch's correction). Two-tailed non-parametric t-tests (Mann-Whitney) were used for Figure S4D. P-values of < 0.05 were taken as significant.

Supplemental references

S1.   Hogan, C., Dupre-Crochet, S., Norman, M., Kajita, M., Zimmermann, C., Pelling, A.E., Piddini, E., Baena-Lopez, L.A., Vincent, J.P., Itoh, Y., et al. (2009). Characterization of the interface between normal and transformed epithelial cells. Nature cell biology *11*, 460-467.

S2.   Ohoka, A., Kajita, M., Ikenouchi, J., Yako, Y., Kitamoto, S., Kon, S., Ikegawa, M., Shimada, T., Ishikawa, S., and Fujita, Y. (2015). EPLIN is a crucial regulator for extrusion of RasV12-transformed cells. Journal of cell science *128*, 781-789.

S3.   Norman, M., Wisniewska, K.A., Lawrenson, K., Garcia-Miranda, P., Tada, M., Kajita, M., Mano, H., Ishikawa, S., Ikegawa, M., Shimada, T., et al. (2012). Loss of Scribble causes cell competition in mammalian cells. Journal of cell science *125*, 59-66.

S4.   Hogan, C., Serpente, N., Cogram, P., Hosking, C.R., Bialucha, C.U., Feller, S.M., Braga, V.M., Birchmeier, W., and Fujita, Y. (2004). Rap1 regulates the formation of E-cadherin-based cell-cell contacts. Molecular and cellular biology *24*, 6690-6700.

S5.   Javaherian, S., D'Arcangelo, E., Slater, B., Zulueta-Coarasa, T., Fernandez-Gonzalez, R., and McGuigan, A.P. (2015). An in vitro model of tissue boundary formation for dissecting the contribution of different boundary forming mechanisms. Integr Biol (Camb) *7*, 298-312.

S6.   Falivelli, G., Lisabeth, E.M., Rubio de la Torre, E., Perez-Tenorio, G., Tosato, G., Salvucci, O., and Pasquale, E.B. (2013). Attenuation of eph receptor kinase activation in cancer cells by coexpressed ephrin ligands. PloS one *8*, e81445.

S7.   Le, T.L., Yap, A.S., and Stow, J.L. (1999). Recycling of E-cadherin: a potential mechanism for regulating cadherin dynamics. The Journal of cell biology *146*, 219-232.

S8.   Kaneko, M., and Nighorn, A. (2003). Interaxonal Eph-ephrin signaling may mediate sorting of olfactory sensory axons in Manduca sexta. The Journal of neuroscience : the official journal of the Society for Neuroscience *23*, 11523-11538.

S9.   Coate, T.M., Swanson, T.L., Proctor, T.M., Nighorn, A.J., and Copenhaver, P.F. (2007). Eph receptor expression defines midline boundaries for ephrin-positive migratory neurons in the enteric nervous system of Manduca sexta. The Journal of comparative neurology *502*, 175-191.

S10.   Dietzl, G., Chen, D., Schnorrer, F., Su, K.C., Barinova, Y., Fellner, M., Gasser, B., Kinsey, K., Oppel, S., Scheiblauer, S., et al. (2007). A genome-wide transgenic RNAi library for conditional gene inactivation in Drosophila. Nature *448*, 151-156.

S11.   Dearborn, R., Jr., He, Q., Kunes, S., and Dai, Y. (2002). Eph receptor tyrosine kinase-mediated formation of a topographic map in the Drosophila visual system. The Journal of neuroscience : the official journal of the Society for Neuroscience *22*, 1338-1349.

S12.   Sarov, M., Barz, C., Jambor, H., Hein, M.Y., Schmied, C., Suchold, D., Stender, B., Janosch, S., Kj, V.V., Krishnan, R.T., et al. (2016). A genome-wide resource for the analysis of protein localisation in Drosophila. eLife *5*.